

Protons Act as a Transmitter for Muscle Contraction in *C. elegans*

Asim A. Beg,^{1,2,3} Glen G. Ernstrom,² Paola Nix,² M. Wayne Davis,² and Erik M. Jorgensen^{1,2,*}

¹Neuroscience Program

²Department of Biology and Howard Hughes Medical Institute
University of Utah, Salt Lake City, UT 84112-0840, USA

³Present address: Columbia University, Center for Neurobiology and Behavior, 630 W. 168th Street, BB1119, New York, NY 10032, USA.

*Correspondence: jorgensen@biology.utah.edu

DOI 10.1016/j.cell.2007.10.058

SUMMARY

Muscle contraction is normally mediated by the release of neurotransmitters from motor neurons. Here we demonstrate that protons can act as a direct transmitter from intestinal cells to stimulate muscle contraction. During the *C. elegans* defecation motor program the posterior body muscles contract even in the absence of neuronal inputs or vesicular neurotransmission. In this study, we demonstrate that the space between the intestine and the muscle is acidified just prior to muscle contraction and that the release of caged protons is sufficient to induce muscle contraction. PBO-4 is a putative Na⁺/H⁺ ion exchanger expressed on the basolateral membrane of the intestine, juxtaposed to the posterior body muscles. In *pbo-4* mutants the extracellular space is not acidified and the muscles fail to contract. The *pbo-5* and *pbo-6* genes encode subunits of a “cys-loop” proton-gated cation channel required for muscles to respond to acidification. In heterologous expression assays the PBO receptor is half-maximally activated at a pH of 6.8. The identification of the mechanisms for release and reception of proton signals establishes a highly unusual mechanism for intercellular communication.

INTRODUCTION

The release of small molecule transmitters is the major mechanism of fast information exchange in the central nervous system. Usually, classical neurotransmitters are stored in synaptic vesicles. Calcium stimulates the fusion of the synaptic vesicles with the plasma membrane and releases the neurotransmitter into the synaptic cleft. The transmitter then binds to ligand-gated ion channels that either excite or inhibit the target cell. However, other neurotransmitters are released via noncanonical mechanisms. For example, gaseous neurotransmitters are not released via synaptic vesicles but pass directly through membranes (Baranano et al., 2001). These unusual properties concealed

the functions of gaseous neurotransmitters for quite some time. There are other candidate molecules that may function as bona fide neurotransmitters but have been set aside due to our incomplete understanding of their biological functions. The proton in particular has properties that make it well suited to play a role in neurotransmission.

Although sparse, hydrogen ions (H⁺) are of enormous biological significance (Kaila and Ransom, 1998). For example, free H⁺ ions can ionize the side groups of proteins and thereby affect the structure and function of proteins. Recently it has been demonstrated that molecules involved in proton signaling are vital for appropriate central nervous system function. Specifically, mouse knockouts have demonstrated that proteins involved in both proton secretion and sensing are required for broad physiological functions that range from pH homeostasis to learning and memory (Bell et al., 1999; Denker et al., 2000; Wemmie et al., 2002; Zha et al., 2006).

To function as an intercellular signal, H⁺ ions must be released from a cell in a regulated way. Na⁺/H⁺ exchangers (NHEs) are ubiquitously expressed proteins capable of regulated release of protons. NHEs catalyze the electroneutral exchange of Na⁺ and H⁺ ions. In general, eukaryotic NHEs transport one Na⁺ ion in and one H⁺ ion out of the cell, thereby alkalinizing the cytoplasm and acidifying the extracellular environment. NHEs are regulated by many distinct signaling molecules, including calmodulin (CaM), phosphatidylinositol 4,5-bisphosphate (PIP₂), and calcineurin homologous protein (CHP) (Aharonovitz et al., 2000; Lin and Barber, 1996; Pang et al., 2001; Wakabayashi et al., 1994, 1997). NHEs have been implicated in numerous physiological processes such as acidification of the intestinal lumen, intracellular pH homeostasis, cell volume regulation, and reabsorption of NaCl across epithelial cells (Counillon and Pouyssegur, 2000; Orłowski, 1993). In addition, some phenotypes suggest that proton secretion may play broader roles in cellular function. For example, NHE1 mutant mice exhibit growth retardation, ataxia, seizures, and defects in cell morphology and adhesion (Bell et al., 1999; Denker et al., 2000). However, it is unclear whether these phenotypes are due to a loss of proton-mediated intercellular signaling or to a side effect of pH misregulation.

If H⁺ ion secretion mediates signals between cells, there must be proton receptors. It is known that protons can modulate neurotransmission. Practically all ligand-gated ion channels are affected by extracellular pH shifts. Ionotropic acetylcholine and

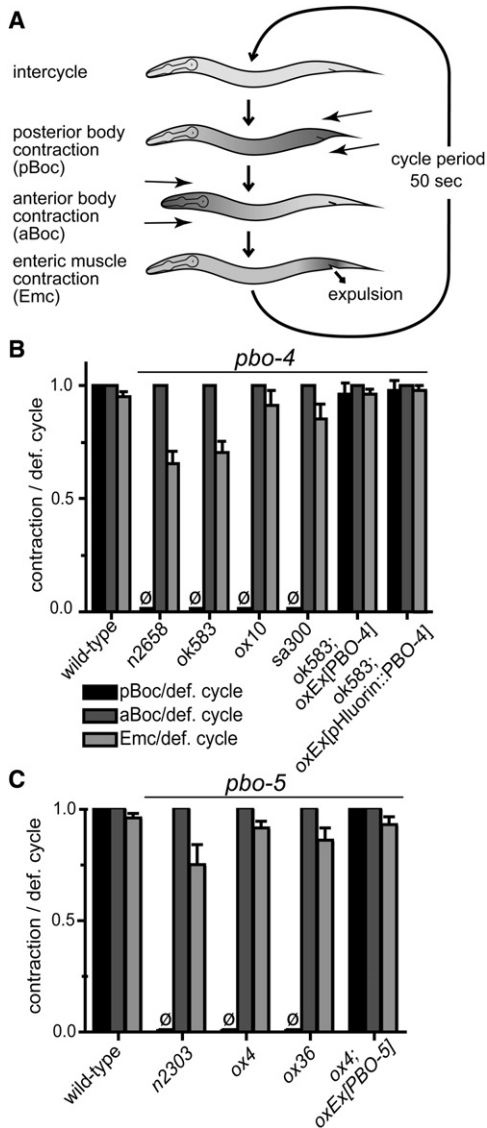


Figure 1. *pbo-4* and *pbo-5* Mutants Lack Posterior Body Contractions

(A) Schematic diagram of the defecation motor program. The defecation motor program occurs every 50 s. First, the posterior body muscles contract in a posterior-to-anterior wave; 3 s later the anterior body muscles contract, followed by contraction of the enteric muscles, which expels the contents of the intestine.

(B) Behavioral characterization of *pbo-4* mutants: *pbo-4* mutants lack the posterior body contraction. Eleven defecation cycles in day 1 adult animals were scored for the presence or absence of each muscle contraction ($n \geq 6$ for each genotype). The *pbo-4* alleles, *n2658*, *ok583*, *ox10*, and *sa300*, exhibited a complete loss of posterior body contractions. In addition, enteric muscle contractions were significantly reduced for *pbo-4(n2658)* and *pbo-4(ok583)* compared to the wild-type (t test, $p < 0.05$). The strain *ok583; oxEx582[PBO-4]* carries an extrachromosomal array containing the genomic *pbo-4* rescuing plasmid (pPD58). The strain *ok583; oxEx584[pHluorin::PBO-4]* contains an array expressing the full-length pHluorin::PBO-4 fusion protein (pAB16). Error bars represent standard error of the mean (SEM).

(C) The *pbo-5* alleles exhibited a loss of posterior body contractions; other motor steps and cycle times were largely normal (wild-type 43.0 ± 1.4 , *n2303*

NMDA receptors are reversibly inhibited by acidic pH and potentiated by alkaline pH (Del Castillo et al., 1962; Giffard et al., 1990; Palma et al., 1991; Traynelis and Cull-Candy, 1990). Conversely, ionotropic GABA receptors are potentiated by acidic pH and inhibited by alkaline pH (Kaila, 1994; Smart and Constanti, 1982; Takeuchi and Takeuchi, 1967). In addition to playing a modulatory role in neurotransmission, protons have been demonstrated to be the major ligand for particular classes of ligand-gated ion channels. Acid-sensing ion channels (ASICs) are members of the ENaC/ Degenerin family of ion channels and are gated by protons (Kaila and Ransom, 1998; Waldmann and Lazdunski, 1998). Some of these channels are involved in monitoring pH in external environments and may act in nociceptive sensory neurons (Krishtal, 2003). Recently, a “cys-loop” family proton-gated ion channel was identified in cyanobacteria that could be involved in adaptation to environmental pH (Bocquet et al., 2007). It is possible that some pH receptors sense internally generated pH changes, since a subset of ASIC receptors are expressed in the central nervous system and mouse mutants lacking ASIC1 exhibit locomotory and dendritic spine defects (Wemmie et al., 2002; Zha et al., 2006). However, it is unclear if protons are released in a physiologically relevant manner to mediate intercellular communication.

Here we demonstrate that H^+ ions act as a transmitter for muscle contraction during the defecation cycle in the nematode *Caenorhabditis elegans*. The defecation cycle is a stereotyped behavior that occurs every 50 s for the life of the animal and is characterized by the coordinated activation of three independent muscle contractions (Croll, 1975; Thomas, 1990). The defecation motor program begins with a sustained contraction of the posterior body muscles; these muscles relax, 3 s later the anterior body muscles contract, and a moment later the enteric muscles contract, expelling the contents of the intestine (Figure 1A). The intestine itself is the timekeeper for the defecation cycle (Dal Santo et al., 1999). The cycle period is set by the activity of the inositol trisphosphate (IP_3) receptor, which regulates release of calcium from storage organelles in the intestine. An anteriorly directed calcium wave directly precedes the motor program and controls the dynamics of the posterior body muscle contraction (Espelt et al., 2005; Norman et al., 2005; Peters et al., 2007).

How might the activity in the posterior intestine direct the contraction of the posterior body muscles? Neither extensive laser ablations of neurons nor mutants in synaptic transmission disrupted the posterior body contraction, suggesting that signaling for this muscle contraction appears to be controlled via a non-neuronal mechanism. To identify the genes required for signaling posterior body contractions, we screened for mutants defective for this motor step (Pbo mutants). In this study, we describe the *pbo-4*, *pbo-5*, and *pbo-6* genes. PBO-4 is most closely related to the mammalian Na^+/H^+ exchanger NHE1 and is localized to the posterior intestine. PBO-5 and PBO-6 encode subunits of a proton-gated cys-loop cation channel. These studies suggest that

40.0 ± 3.9 , *ox4* 41.2 ± 6.1 , *ox36* 38.7 ± 7.1 , rescue: 42.8 ± 5.6). The strain *ox4; oxEx599* is *pbo-5(ox4)* carrying an extrachromosomal array containing the *pbo-5* minigene rescuing plasmid (pAB18). Error bars represent SEM.

H⁺ ions act as a primary transmitter that activates the posterior body contraction during the defecation cycle in *C. elegans*.

RESULTS

pbo-4 and *pbo-5* Mutants Specifically Lack the Posterior Body Contraction

Calcium is released from intracellular stores in the intestinal cells immediately before the posterior body contraction of the defecation cycle, suggesting that this calcium spike might initiate the behavioral program (Dal Santo et al., 1999). During locomotion, all body muscles are stimulated by acetylcholine motor neurons. As expected, mutants lacking acetylcholine synthesis (*cha-1*, choline acetyltransferase) are paralyzed; however, these animals exhibit perfectly normal posterior body contractions (posterior body contractions/cycle: ChAT *cha-1(b401ts)42/43*). Furthermore, mutations that disrupt synaptic vesicle fusion (*unc-13*) or dense core vesicle fusion (*unc-31/CAPS*) result in animals that are also paralyzed but still have normal posterior body contractions (*unc-13(s69) 46/49*; *CAPS unc-31(e928)87/87*). Finally extensive laser ablations failed to identify any neuron that contributed to the initiation of posterior body contraction, suggesting that this behavior is mediated via a non-neuronal mechanism (E.M.J. and H.R. Horvitz, unpublished data).

To identify components of the signaling pathway required for posterior body contraction, we screened for mutants defective in this motor step. Recessive mutations in two genes, *pbo-4* and *pbo-5*, specifically eliminate this step in the motor program (Figures 1B and 1C). Importantly, locomotion is normal in both *pbo-4* and *pbo-5* mutants. Because locomotion and posterior body contraction rely on the same muscles, the lack of muscle contraction during the defecation cycle in *pbo-4* and *pbo-5* mutants is not a result of degeneration or a developmental defect in the posterior body muscles.

PBO-4 Encodes a Putative Na⁺/H⁺ Exchanger

The *pbo-4(n2658)* allele was mapped by standard two and three factor mapping and the *pbo-4* gene identified by microinjection rescue. The cosmid K09C8 rescued the phenotype of *n2658* and *ok583* mutants, and an 8.5 kb subclone fragment containing only the K09C8.1 open-reading frame was sufficient to rescue the posterior body contraction defect in *ok583* mutants (Figure S1A). To confirm the identity of *pbo-4*, we sequenced genomic DNA from mutants and found mutations within the K09C8.1 open-reading frame in each *pbo-4* allele (Figure S1A and Table S1). The K09C8.1 gene is also known as *nhx-7* (Nehrke and Melvin, 2002), but for clarity we refer to it as *pbo-4*.

The cDNA of *pbo-4* encodes a predicted 783 amino acid protein (Figure S2) that is homologous to Na⁺/H⁺ exchangers. Plasma membrane Na⁺/H⁺ ion exchangers mediate the electro-neutral exchange of one Na⁺ ion into the cell for one H⁺ ion out of the cell and, thus, increase intracellular pH while acidifying the extracellular space. Na⁺/H⁺ ion exchangers are multidomain proteins containing an intracellular N-terminal domain, 12 transmembrane domains, and an intracellular carboxy terminal tail (Figures S1B and S2) (Wakabayashi et al., 2000). NHEs can be subdivided into separate families and are distinguished by their subcellular localization and regulatory mechanisms. PBO-4

shares the highest sequence identity with NHE1 (26% identity) and, conversely, the closest homolog to NHE1 in the *C. elegans* genome is PBO-4. PBO-4 also shares relatively high sequence identity with NHE2 and NHE3 (22% and 21%, respectively). The carboxy-terminal domain is not well conserved among the diverse members of the Na⁺/H⁺ ion exchanger family, and each member contains distinct modulatory sites that greatly affect transport activity. For example, the carboxy terminus of NHE1 contains PIP₂-binding domains, a calmodulin (CaM)-binding domain, and numerous phosphorylation sites, whereas NHE3 lacks the PIP₂- and calmodulin-binding domains (Orlowski and Grinstein, 2004). Similar to NHE1, the carboxy tail of PBO-4 contains a predicted PIP₂-binding domain, a CaM-binding domain, and CamKII and PKC phosphorylation sites (Figure S2).

PBO-4 Is Expressed in the Posterior Intestine

The defect in the posterior body contractions in mutants suggested that PBO-4 would be expressed in either the posterior body muscles, where the defect occurs, or in the intestine, where the defecation clock resides (Dal Santo et al., 1999). We generated a transgene with superecliptic pHluorin GFP (pHluorin) inserted into the N-terminal domain of PBO-4 and expressed it in *pbo-4(ok583)* mutants. pHluorin is a pH-sensitive form of GFP whose fluorescence is quenched by acidic media (Miesenbock et al., 1998), and the superecliptic form is a version of pHluorin with enhanced pH sensitivity (Sankaranarayanan and Ryan, 2000). The pHluorin::PBO-4 fusion protein rescued the posterior body contraction defect of the mutants, demonstrating that the protein was functional and properly localized (Figure 1B). The fluorescently tagged protein was expressed on the basolateral surface of the intestine, exclusively in the most posterior intestinal cells (Figure 2A), consistent with previous observations (Nehrke and Melvin, 2002). To confirm basolateral expression, we exposed the posterior intestine in situ—without exposing the apical, luminal surface—to acidic media, which quenched the majority of the pHluorin::PBO-4 fluorescence (Figure S3). The expression pattern of PBO-4 demonstrates that the protein resides on the basolateral surface of the intestine, appropriately localized to release a signal from the intestine to the posterior body wall muscles. Electron micrographs of the posterior intestine-muscle interface demonstrate that muscle arms extend from the posterior muscles and form intestino-muscular junctions (Figure 2B).

To further demonstrate that PBO-4 functions in the intestine, we rescued *pbo-4(n2658)* with the pHluorin::PBO-4 fusion driven by the promoter from the vitellogenin gene *vit-2*, which is expressed in all intestinal cells. Vitellogenin is synthesized in the intestine and transported to oocytes, where it serves to provide essential nutrients to the developing embryo. Because vitellogenins are only required in mature oocytes, we found that L4 animals were not rescued by this construct, while 1-day-old adults were almost fully rescued (Figure 3). This result demonstrates that PBO-4 is required solely in intestinal cells, and that the *pbo-4* defect is due to an acute loss of signaling function, not due to a developmental defect in the intestine.

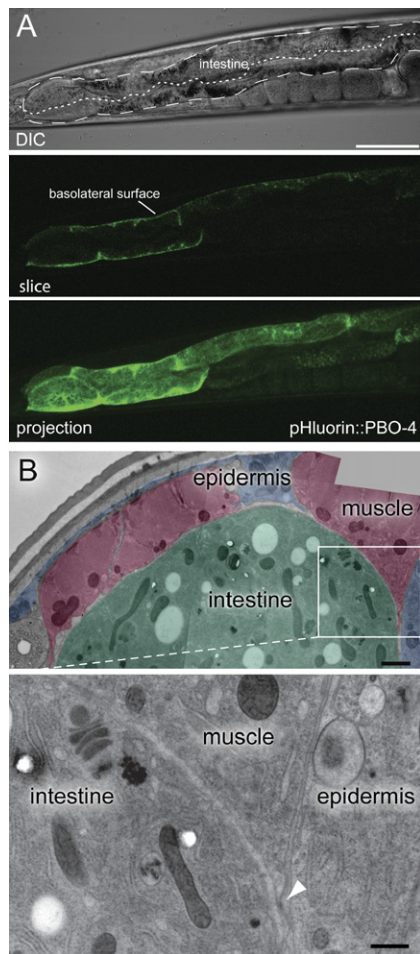


Figure 2. The PBO-4 Na^+/H^+ Exchanger Is Expressed on the Surface of the Intestine

(A) Confocal images of transgenic animals expressing the pHluorin::PBO-4 fusion protein. DIC (top), confocal slice (middle), and confocal projection (bottom) of an adult hermaphrodite expressing the GFP fusion protein. Fluorescence was observed on the basolateral surface of the posterior intestine cells only. Animals carrying this fusion protein were rescued for posterior body contractions (*pbo-4(ok583); oxEx584*), demonstrating that the fusion protein is functional and properly localized. The dashed lines indicate the intestinal boundary in the DIC image. Scale bar is 50 μM .

(B) Top panel shows cross-sectional electron micrograph of the posterior end of a wild-type *C. elegans* adult hermaphrodite (top). The intestine (green), muscle (red), and epidermis (blue) are pseudocolored, and the region of interest is denoted by a white box. Scale bar is 1 μm . Bottom panel shows closeup of the region of interest. Note the muscle extends a process to form a long muscle-intestinal interface (arrowhead). Scale bar is 0.5 μm .

Acidification of the Coelomic Space Precedes Posterior Contraction

Since the posterior body contraction is not mediated by classical neurotransmitters or peptides it is possible that acidification of the coelomic space by PBO-4 may stimulate contraction of the posterior body muscles. To visualize such a signal, we used superecliptic pHluorin, a pH-sensitive GFP whose fluorescence exhibits a pK_a of pH 7.1 and is quenched at low pH (Miesenbock et al., 1998; Sankaranarayanan and Ryan, 2000). The superecliptic

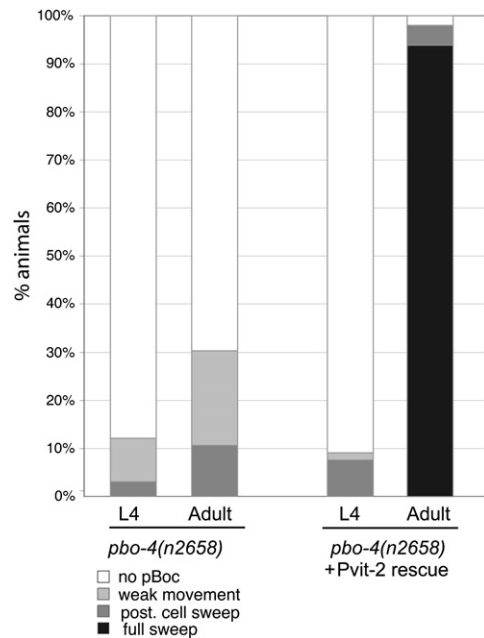


Figure 3. *pbo-4* Functions Cell Autonomously in the Intestine

pbo-4(n2658) animals have no or very weak posterior body contractions. When the wild-type pHluorin::PBO-4 transgene is expressed under the *vit-2* promoter, it rescues the *pbo-4* phenotype in young adults (*pbo-4(n2658); oxEx770[Pvit-2::pHluorin::PBO-4]*). The *vit-2* promoter is expressed only in the intestinal cells in the adult stage. Animals were scored as having no posterior body movement (no pBoc), weak movement of the tail, a contraction that only sweeps the length of the posterior intestinal cell, or a full posterior body contraction that sweeps from the tip of the tail to almost the vulva.

tic pHluorin was inserted into the first extracellular loop of PBO-4 (pHluorin::PBO-4) to monitor extracellular pH (Figures S1B and S2). If dissected intestines were exposed to acidic media, fluorescence was rapidly quenched demonstrating that the pH sensor was on the surface (Figure S3). To determine whether the posterior coelomic space was acidified *in vivo* prior to a posterior body contraction, we glued worms to agar but left the tip of the tail free to observe muscle contractions. Rapid fluorescence quenching always preceded the posterior body contraction (Figures 4A and 4D and Movie S1). Fluorescence spikes were characterized by a steep rise to peak ($\tau = 1.9 \pm 0.09$ s, $n = 18$ recordings from separate animals; 10%–90% of peak), and a slower exponential decay to baseline fluorescence ($\tau = 2.9 \pm 0.3$ s, $n = 18$) and preceded the muscle contraction with a latency of approximately 2 s (Figures 4E–4H).

To test whether PBO-4 is fully required for the acidification, we deleted the C-terminal tail of the pHluorin::PBO-4 transgene to generate a nonrescuing fusion (pHluorin::PBO-4(ΔC)). This truncated construct expressed in the posterior intestinal cells, but there were very few, if any, fluorescence transients. In 5 of 14 animals with the truncated construct no transients were detected. The remaining nine animals possessed significantly reduced transients ($\Delta\text{F}/\text{F} = 5.0\% \pm 0.7\%$, $n = 18$ for pHluorin::PBO-4 versus $\Delta\text{F}/\text{F} = 1.0\% \pm 0.2\%$, $n = 14$ for truncated pHluorin::PBO-4(ΔC), $p < 0.0001$) that were quantitatively and qualitatively distinct from the rescuing pHluorin reporter (Figures 4B and 4E–4H).

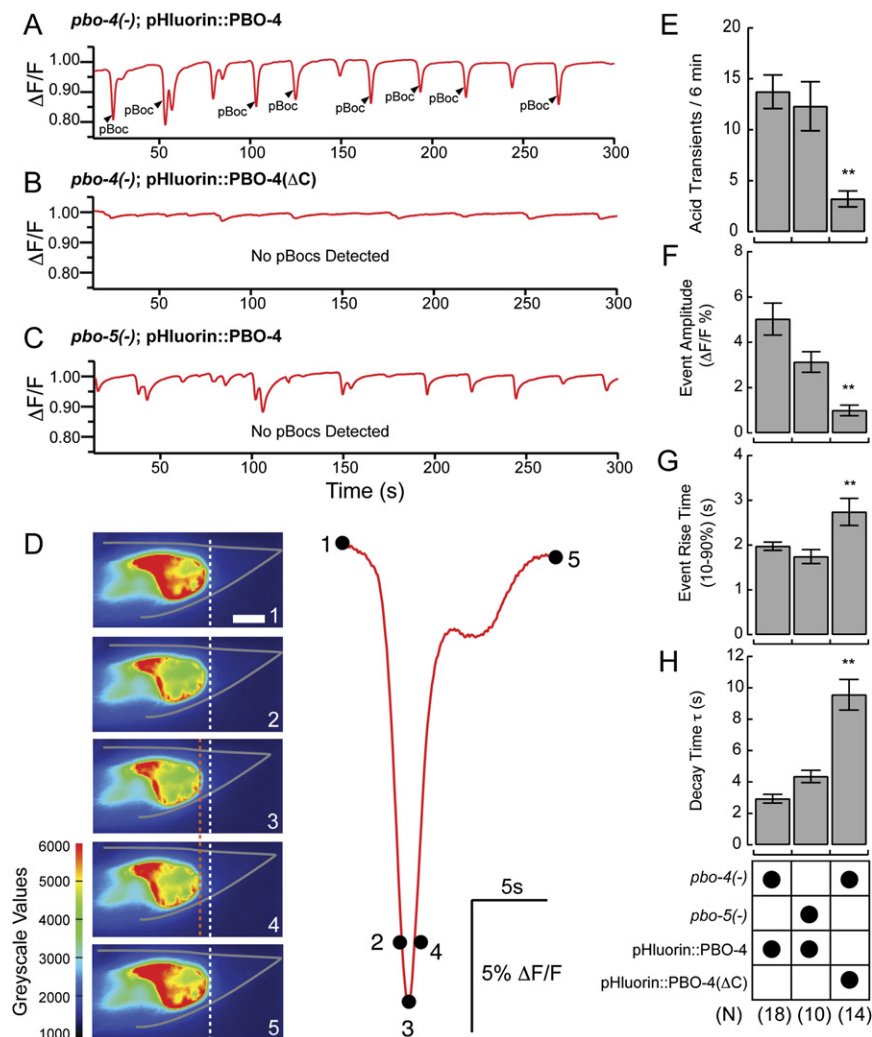


Figure 4. Acidification Precedes Posterior Body Contractions

(A–C) Extracellular pH changes were measured using pHluorin expressed on the basolateral surface of the posterior intestine (pHluorin::PBO-4). In (A), acidification transients were observed in a *pbo-4* rescued strain (EG3326 *pbo-4(ok583); oxEx584[pHluorin::PBO-4(+)]*). The arrowhead denotes distinct accordion-like posterior body contractions (pBoc) observed following a transient drop in fluorescence. In (B), acidification transients were reduced in a *pbo-4(-)* strain (EG4176 *pbo-4(n2658); oxEx782[pHluorin::PBO-4(ΔC)]*). The carboxy terminus of PBO-4 is deleted in the PBO-4(ΔC) construct, and it does not rescue posterior body contractions in the mutant strain. In (C), no posterior body contractions were detected in a mutant lacking the acid receptor subunit PBO-5 (EG4178 *pbo-5(ox4); oxEx784[pHluorin::PBO-4(+)]*). Acid transients produced by the pHluorin::PBO-4 transgenic protein were observed with similar kinetics and frequency as in (A).

(D) Image sequence of the first acid transient corresponding to the first event in (A), expanded on the right. The white dashed line indicates the initial location of the posterior intestine at the start of the pH decrease. The orange line indicates the anterior displacement and eventual posterior relaxation of the posterior body contraction. Fluorescence intensity is pseudocolored to highlight differences. Scale bar (0.02 mm), grayscale pixel intensity values in arbitrary units. Traces in (A)–(C) are mean pixel intensity recordings from individual animals; regions of interest were defined by hand-drawn areas slightly larger than the fluorescent region of the posterior intestine.

(E) The number of transients in a 6 min recording were significantly fewer in the pHluorin::PBO-4(ΔC) strain (3.2 ± 0.8 , $n = 14$) compared to *pbo-4(-); pHluorin::PBO-4* (13.7 ± 1.6 , $n = 18$, $p < 0.001$) and *pbo-5(-); pHluorin::PBO-4* (12.3 ± 2.4 , $n = 10$, $p < 0.01$).

(F) Average transient amplitude per individual was significantly smaller in the *pbo-4(-)* pHluorin::PBO-4(ΔC) strain ($3.1 \pm 0.5\%$ ΔF/F, $n = 10$) compared to *pbo-4(-); pHluorin::PBO-4(+)* ($5.0\% \pm 0.7\%$ ΔF/F, $n = 18$, $p < 0.0001$) and *pbo-5(-); pHluorin::PBO-4(+)* ($3.1\% \pm 0.5\%$ ΔF/F, $n = 10$, $p = 0.0012$).

(G) Average transient rise times were significantly slower in the *pbo-4(-)* pHluorin::PBO-4(ΔC) strain (2.7 ± 0.3 s, $n = 9$) compared to *pbo-4(-); pHluorin::PBO-4(+)* (1.9 ± 0.09 s, $n = 18$, $p = 0.01$) and *pbo-5(-); pHluorin::PBO-4(+)* (1.7 ± 0.2 s, $n = 10$, $p = 0.01$).

(H) Average transient decay times were significantly slower in the *pbo-4(-)* pHluorin::PBO-4(ΔC) strain (9.6 ± 1.0 s, $n = 9$) compared to *pbo-4(-); pHluorin::PBO-4(+)* (2.9 ± 0.3 s, $n = 18$, $p < 0.001$) and *pbo-5(-); pHluorin::PBO-4(+)* (4.3 ± 0.4 s, $n = 10$, $p < 0.001$).

No statistical significance in any of these parameters were found between *pbo-4(-); pHluorin::PBO-4(+)* and *pbo-5(-); pHluorin::PBO-4(+)* strains. Asterisks indicate statistical significance between *pbo-4(-); pHluorin::PBO-4(ΔC)* and *pbo-4(-); pHluorin::PBO-4(+)* strains. N is the number of 6 min recordings made from individual animals. Bars indicate mean \pm SEM. The Mann-Whitney statistical test was used for (B) and (C); t tests were used for (A) and (D).

PBO-4(ΔC) strain ($1.0\% \pm 0.2\%$ ΔF/F, $n = 14$) compared to *pbo-4(-); pHluorin::PBO-4(+)* ($5.0\% \pm 0.7\%$ ΔF/F, $n = 18$, $p < 0.0001$) and *pbo-5(-); pHluorin::PBO-4(+)* ($3.1\% \pm 0.5\%$ ΔF/F, $n = 10$, $p = 0.0012$). No transients were detected in 5/14 *pbo-4(-); pHluorin::PBO-4(ΔC)* individuals.

(G) Average transient rise times were significantly slower in the *pbo-4(-)* pHluorin::PBO-4(ΔC) strain (2.7 ± 0.3 s, $n = 9$) compared to *pbo-4(-); pHluorin::PBO-4(+)* (1.9 ± 0.09 s, $n = 18$, $p = 0.01$) and *pbo-5(-); pHluorin::PBO-4(+)* (1.7 ± 0.2 s, $n = 10$, $p = 0.01$).

(H) Average transient decay times were significantly slower in the *pbo-4(-)* pHluorin::PBO-4(ΔC) strain (9.6 ± 1.0 s, $n = 9$) compared to *pbo-4(-); pHluorin::PBO-4(+)* (2.9 ± 0.3 s, $n = 18$, $p < 0.001$) and *pbo-5(-); pHluorin::PBO-4(+)* (4.3 ± 0.4 s, $n = 10$, $p < 0.001$). No statistical significance in any of these parameters were found between *pbo-4(-); pHluorin::PBO-4(+)* and *pbo-5(-); pHluorin::PBO-4(+)* strains. Asterisks indicate statistical significance between *pbo-4(-); pHluorin::PBO-4(ΔC)* and *pbo-4(-); pHluorin::PBO-4(+)* strains. N is the number of 6 min recordings made from individual animals. Bars indicate mean \pm SEM. The Mann-Whitney statistical test was used for (B) and (C); t tests were used for (A) and (D).

and Movie S2). The small changes in pH remaining in this strain could represent residual activity of the truncated PBO-4 protein or activity from another Na^+/H^+ ion exchanger such as NHX-6, which is also expressed in the intestine (Nehrke and Melvin, 2002). Thus, PBO-4 is required for the transient acidification of the extracellular space that precedes posterior body contractions.

To test whether the fluorescent events were merely artifacts produced by the posterior body contractions, the reporter construct was introduced into the *pbo-5(ox4)* mutant that fails to execute posterior body contractions. In *pbo-5* mutants, fluo-

rescence transients were detected with similar frequency, amplitude, and kinetics as in the wild-type background, indicating that fluorescence transients cannot be attributed to posterior body contraction motion (Figures 4C and 4E–4H).

pbo-5 Encodes a Ligand-Gated Ion Channel

Because *pbo-5* mutants retain the pH transient but lack a posterior body contraction, it is likely that the *pbo-5* gene product acts downstream of PBO-4, possibly as part of the pH sensing pathway in the muscle. The *pbo-5* gene was mapped to a small region on the right arm of chromosome V by standard two and

three factor mapping (Figure S4A). The posterior body contraction defect observed in *pbo-5(n2303)* mutants was rescued by injection of a yeast artificial chromosome (YAC) Y44A6 containing *C. elegans* genomic DNA from this region. To further localize the rescuing activity, a series of deletions were made from the Y44A6 YAC and injected into *pbo-5(n2303)* animals (Figure S4A). In addition, we analyzed the breakpoints of several chromosome V terminal deletions. From these experiments rescuing activity was localized to a single predicted open reading frame, Y44A6E.1 (Figure S4B). To demonstrate *pbo-5* was encoded by Y44A6E.1, we constructed a minigene composed of genomic DNA containing 4.2 kb of promoter sequences and exons 1 and 2; exon 2 was fused to the rest of the open-reading frame using sequences from a cDNA. Animals carrying this plasmid were fully rescued for posterior body contraction (Figure 1C, *ox4; ox-Ex[PBO-5]*). Additionally, we sequenced 20 *pbo-5* alleles and found mutations within the Y44A6E.1 open-reading frame in all of them (Figure S4C and Table S2). The *pbo-5* mutations fall into four categories: (1) nine terminal deletions, (2) three nonsense mutations, (3) seven missense mutations, and (4) one splice junction mutation (Table S2). The predicted *pbo-5* cDNA encodes a 504 amino acid protein.

The primary structure of the *pbo-5* cDNA was determined by reverse transcription and polymerase chain reaction (RT-PCR). The *pbo-5* cDNA includes an SL1 *trans*-spliced leader sequence at the 5' end and a total of nine exons spanning a 7 kb genomic region (Figure S4C). BLAST and protein motif queries of PBO-5 demonstrated that the predicted protein is a subunit of the cys-loop ligand-gated ion channel superfamily. Each member of the cys-loop protein family contains a signal peptide, an extracellular amino terminus that contains consensus ligand-binding sites and an invariant disulfide bonded loop (the cys-loop), four transmembrane domains (M1-M4), a large cytoplasmic loop between M3-M4, and a short extracellular carboxy terminus (Karlín and Akabas, 1995; Ortells and Lunt, 1995) (Figure S5). Electron microscopy and electrophysiological and structural data suggest that cys-loop ligand-gated ion channels are formed from five homologous subunits that are pseudosymmetrically arranged around a central ion channel, such that the M2 domain lines the ion-channel wall and determines ion selectivity (Betz, 1990; Brejc et al., 2001; Unwin, 1993). Hydrophathy plots and alignment of PBO-5 with various ligand-gated ion channel subunits demonstrates that PBO-5 contains the necessary features of a cys-loop ligand-gated ion channel subunit (Figure S5).

Although many cys-loop ligand-gated ion channel subunits have been identified, these subunits can usually be assigned to one of four neurotransmitter receptor families based on sequence similarity: the acetylcholine, serotonin, glycine, or GABA families. Phylogenetic analysis demonstrates that PBO-5 represents a divergent subunit that cannot be categorized into one of the four families based on sequence similarity (Figure S6). Analysis of residues that determine ligand interactions did not identify a potential ligand for the PBO-5 receptor (Figure S5). Furthermore, mutants that are defective in GABA, acetylcholine, serotonin, and peptidergic transmission do not exhibit posterior body contraction defects. Therefore, it is unlikely that PBO-5 is activated by known classical neurotransmitters.

PBO-6 Is Homologous to PBO-5

Because cys-loop receptors are composed of homo- or heteropentamers, we scanned the genome to identify candidate proteins that may be required to form a functional receptor with PBO-5. Only one other gene, F11C7.1, which we call *pbo-6*, is closely related to *pbo-5* (Figures S5 and S6). To determine the primary structure of PBO-6 we performed RT-PCR and isolated full-length cDNA clones. The full-length cDNA consists of 13 exons that span 4.1 kb of the genome. The PBO-6 cDNA encodes a 423 amino acid protein that shares 35% sequence identity with PBO-5 (Figure S5). The residues in the pore-forming M2 domains are identical with the exception of one conservative amino acid change. The *C. elegans* knockout consortium isolated a 1.9 kb deletion allele of *pbo-6*, removing residues 118–310, which encompasses the majority of the N terminus and transmembrane domains M1-M3 and is therefore likely to be a null allele. Surprisingly, *pbo-6(ok1564)* animals exhibit normal posterior body contractions (66 pBocs /66 defecation cycles, $n = 6$), suggesting PBO-6 is not critical for the execution of the posterior body contraction *in vivo*.

PBO-5 and PBO-6 Are Expressed in the Posterior Body Wall Muscles

If PBO-5 and PBO-6 are subunits of the receptor that mediates the posterior body contraction, then they should be expressed in the posterior body muscles. To determine the cellular expression of *pbo-5*, a transcriptional fusion gene was constructed that contained 3.8 kb upstream sequence of the translational start codon fused to the GFP open-reading frame. To establish the expression pattern of PBO-6, we built a transcriptional fusion gene containing 4 kb of upstream promoter sequence fused to GFP. Animals carrying either the PBO-5 or PBO-6 transgene expressed GFP in the most-posterior body muscles (Figure 5), confirming these subunits are localized to the appropriate tissues to mediate posterior body muscle contraction.

PBO-5/6 Forms a Proton-Gated Ion Channel

To determine if PBO-5 and PBO-6 can assemble or coassemble to form a functional receptor, we injected PBO-5 and PBO-6 cRNA alone or in combination into *Xenopus* oocytes. Agonists for other ligand-gated ion channels (ACh, GABA, glycine, 5-HT, glutamate, and choline) did not activate PBO-5, PBO-6, or PBO-5/6 injected eggs (data not shown). Failure of these neurotransmitters to activate the receptors was not unexpected as genetic evidence demonstrates that neither acetylcholine, GABA, glutamate, nor serotonin is required for the posterior body contraction.

We tested if H^+ ions were capable of activating PBO-5-, PBO-6-, or PBO-5/6-injected oocytes. Test pulses of pH 6.0 did not elicit detectable currents from oocytes injected with PBO-6 cRNA alone (Figure 6A). Slight currents were detected when pH 6.0 test pulses were applied to PBO-5 injected oocytes, suggesting that PBO-5 can form a homomeric channel ($-0.18 \pm 0.06 \mu A$, $n = 18$) (Figure 6A). This may explain the lack of an obvious phenotype in *pbo-6* mutants. By contrast, PBO-5/6-injected eggs exhibited extremely robust currents when a pH 6.0 test pulse was applied ($-3.9 \pm 0.35 \mu A$, $n = 18$) (Figure 6A). These data suggest that PBO-5/6 heteromultimerization is required

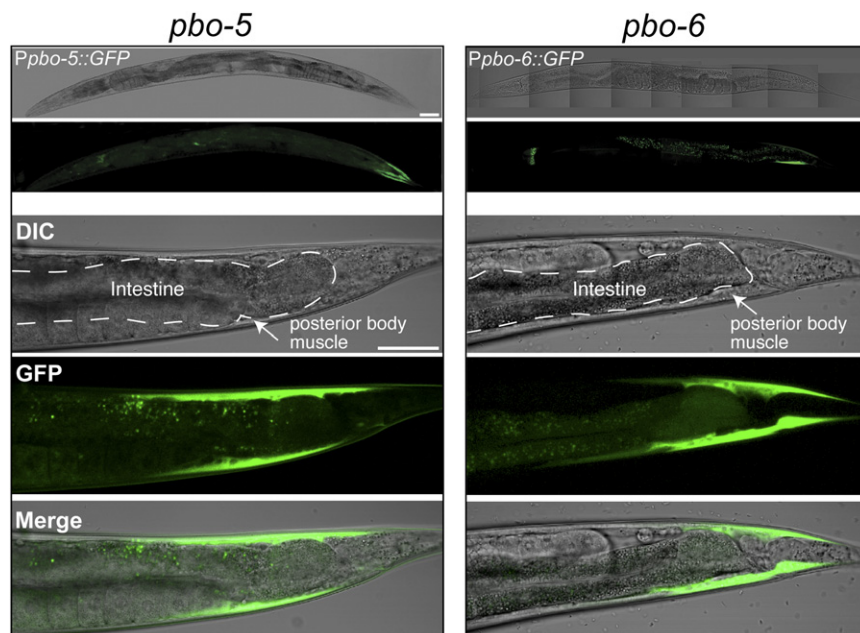


Figure 5. Expression Pattern of *pbo-5* and *pbo-6*

Confocal images of adult animals expressing GFP fusion genes. The animals are oriented with anterior to the left and posterior to the right. Shown in left panels is an animal expressing the *pbo-5* transcriptional GFP fusion protein. Shown in right panels is an animal expressing the *pbo-6* transcriptional GFP fusion protein. Note that *pbo-5* and *pbo-6* have overlapping expression in the posterior body muscles. In addition, *pbo-5* is expressed in the head neurons RIFL, RIFR, and RIS (data not shown). Anterior fluorescence in the top *pbo-6* image is autofluorescence. The intestine of the animals is noted by a dashed white line. Arrows mark the posterior body muscle in the DIC image. Top, DIC; middle, epifluorescence; bottom, merged image. Scale bar is 50 μm .

for efficient functional receptor expression in vitro. To demonstrate current responses evoked by changes in pH were not due to endogenous channels or transporters, we applied maximal test pulses of pH 6.0 to naive oocytes or oocytes injected with water ($n > 30$). Only oocytes injected with PBO-5 or PBO-5/6 cRNA exhibited H^+ -gated responses, while uninjected cells exhibited no inward current in response to pH 6.0 test pulses.

To measure the pH_{50} (half-maximal activation) of putative PBO-5/6 heteromultimers, we first identified the pH range at which the recombinant receptors were activated. We determined that the pH_{10} (10% maximal activation) was approxi-

mately pH 7.0. The perfusion buffer was set at pH 7.4 for all experiments, where no activation of recombinant receptors was observed. A pH_{50} of 6.83 ± 0.01 was determined by applying decreasing pH test pulses (pH 7.2–6.0). A steep Hill coefficient of 5 suggests that PBO-5/6 receptors exhibit significant H^+ ion binding cooperativity (Figures 6B and 6C).

H^+ ions have been demonstrated to modulate classical synaptic transmission. For example, acidic changes inhibit acetylcholine receptor function, whereas alkaline environments enhance receptor function (Palma et al., 1991). Although none of the classical neurotransmitters tested could activate the PBO-5/6 receptor on their own, we sought to determine whether classical neurotransmitters coactivate PBO-5/6 receptors. Application

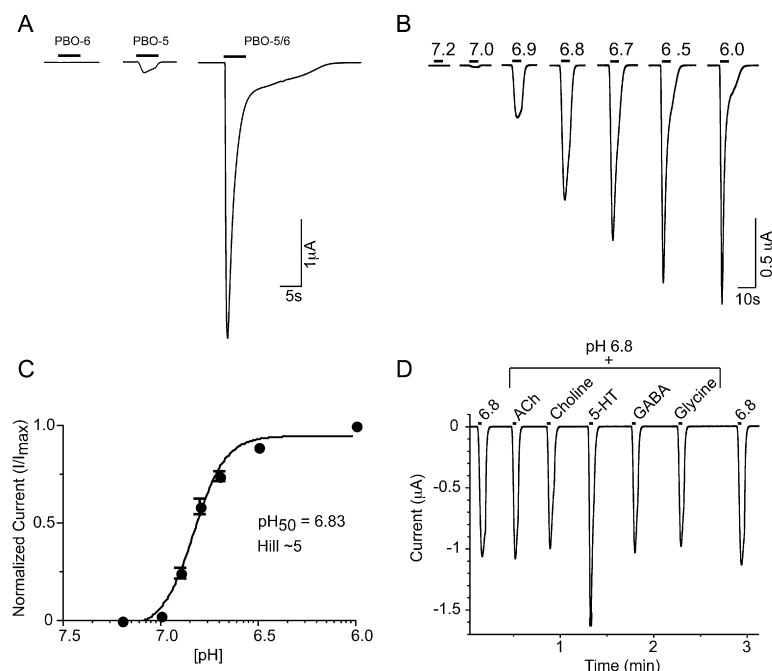


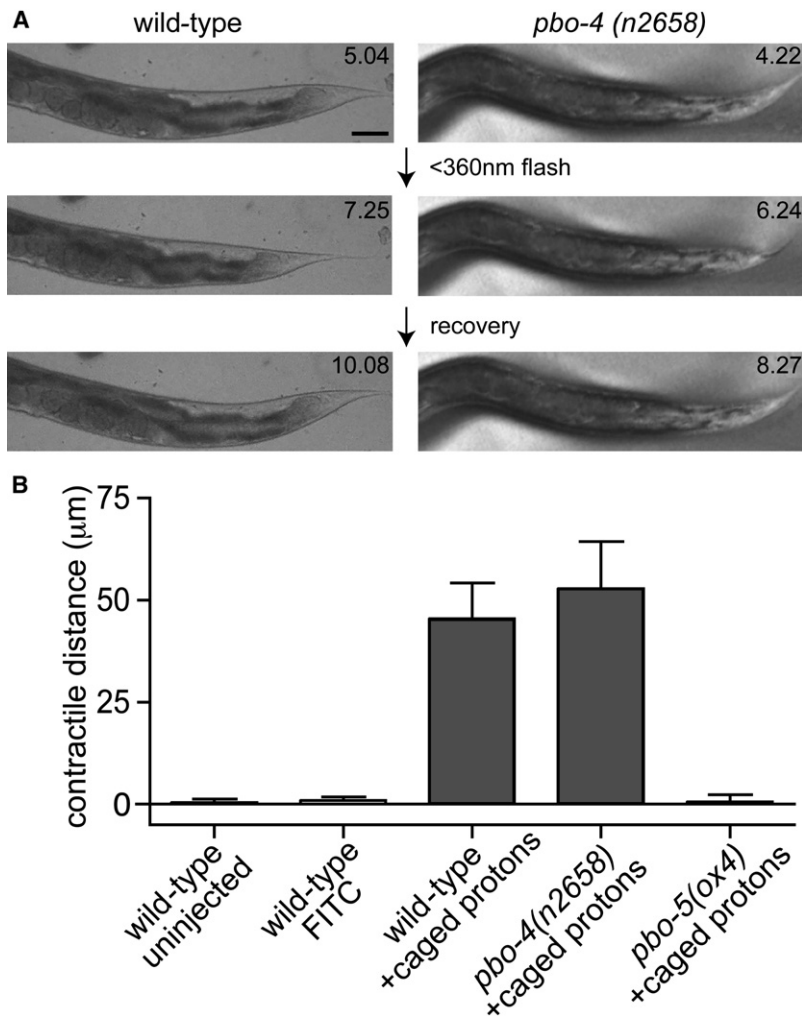
Figure 6. PBO-5/6 Form a Heteromultimeric H^+ -Gated Ion Channel

(A) Representative traces of PBO-6-, PBO-5-, and PBO-5/6-injected oocyte responses to a pH 6.0 test pulse for 5 s (black bar). PBO-6-injected eggs never exhibited a functional response to pH 6.0 application. PBO-5-injected oocytes exhibited a slight response with a mean current amplitude = $-0.18 \pm 0.06 \mu\text{A}$. PBO-5/6 coinjected oocytes had robust response to pH 6.0 with a mean current amplitude = $-3.9 \pm 0.35 \mu\text{A}$. Eighteen oocytes total from six different batches were tested for each condition.

(B) Representative traces of PBO-5/6 dose-response experiments. pH and duration of applied solution is shown above each trace.

(C) PBO-5/6 pH dose-response curve. PBO-5/6-expressing oocytes were voltage clamped at -60 mV , and a series of test pH applications (7.2–6.0) were bath applied for 5 s. Each point represents the mean current value normalized to the maximum and minimum values. A pH_{50} of 6.83 ± 0.01 and a Hill coefficient of 5.0 were determined for PBO-5/PBO-6 receptors ($n = 18$). Error bars represent SEM.

(D) H^+ ions are sufficient to activate PBO-5/6 receptors. A representative coactivation experiment is shown. All points are in response to a pulse of pH 6.8 with or without the addition of 1 mM neurotransmitter. Cells were voltage clamped at -60 mV .



of pH 6.8 solution plus 1mM acetylcholine, choline, GABA, or glycine were not significantly different from pH 6.8 only application (Figure 6D). However, coapplication of 5-HT did result in a small but significant increase in amplitude compared to controls (Figure 6D). Thus, the activity of the PBO receptor can be modulated by serotonin, although H^+ ions alone are sufficient to activate the PBO receptor.

Uncaging Protons Evokes a Posterior Body Contraction

Acidification of the cleft could activate the posterior body contraction directly; alternatively, H^+ ions may act as a secondary transmitter in alliance with another molecule. If H^+ ions are sufficient to activate the posterior body contraction then application of exogenous H^+ ions should be able to induce a posterior body contraction. We injected caged protons into the coelomic space of wild-type worms. After recovery and mounting for observation, the animals received a brief flash of light (<360 nm for 1–2 s) to uncage the protons. Injected animals exhibited a flash-induced posterior body contraction ($45.4 \pm 8.8 \mu\text{m}$, $n = 11$) that was in phase with the flash stimulus (Figure 7A). Importantly, uninjected controls and FITC-dextran injected controls failed to activate a perceptible posterior body contraction in response

Figure 7. H^+ Ions Activate the Posterior Body Contraction

(A) Flash uncaging of H^+ ions can activate the posterior body contraction in vivo. In the left panels are the wild-type: top, the tail of an adult animal before uncaging; middle, the same animal after a flash of UV light was applied for 1–3 s. bottom, the same animal 3 s after the flash. The posterior body muscles have relaxed after the flash stimulus. In the right panels are *pbo-4(sa300)*: top, the tail of a *pbo-4* mutant before the flash stimulus; middle, a flash-induced posterior body contraction is observed in mutant animals, demonstrating that H^+ ions can bypass the *pbo-4* defect to activate the posterior body contraction; bottom, *pbo-4(n2658)* mutants relax the posterior body muscles after the flash-induced contraction. All animals were injected with 0.1 mg/ml of NPE caged- H^+ ions. Scale bar is 50 μm .

(B) Quantification of flash-induced posterior body contractions. Controls included uninjected wild-types, FITC-injected wild-types, and uninjected *pbo-4(n2658)* animals (not shown). Control animals fail to activate a posterior body contraction upon flash uncaging of H^+ ions. Wild-type and *pbo-4(n2658)* animals injected with caged protons exhibited a mean contractile distance of $45.4 \pm 8.86 \mu\text{m}$ ($n = 11$) and $52.82 \pm 11.45 \mu\text{m}$ ($n = 7$), respectively. *pbo-5(ox4)* lacks a subunit of the PBO proton receptor that is required for posterior body contractions. Uncaging H^+ ions was unable to stimulate muscle contraction in this strain. Error bars represent SEM.

to the light stimulus (Figure 7B). These results demonstrate that H^+ ions can activate the posterior body contraction in vivo.

Although these data demonstrate that acidification can stimulate muscle contraction, they do not eliminate the possibility that *pbo-4* provides some other essential component. To determine whether *pbo-4* is specifically defective

in proton secretion, we demonstrated that uncaging of H^+ ions bypasses the requirement for PBO-4. We injected *pbo-4* mutants with caged protons and released them by flash photolysis. *pbo-4* mutants normally do not initiate posterior body contractions (Figure 1B); however, when injected *pbo-4* mutants were subjected to uncaging of H^+ ions we observed posterior body contractions ($52.8 \pm 11.5 \mu\text{m}$, $n = 7$) that were in phase with the flash stimulus (Figure 7B). The flash-induced posterior body contractions appeared identical to those induced in the wild-type and were not significantly different in mean contractile distance compared to wild-type injected animals (t test, $p < 0.05$). Finally, it was possible that H^+ ions were causing a contraction through a toxic response rather than acting as a transmitter. However, uncaging of H^+ ions in *pbo-5(ox4)* failed to elicit a posterior body contraction (Figure 7B). Thus, H^+ ions are activating a specific receptor on the surface of the muscles, rather than causing a contraction by damaging cells.

DISCUSSION

Mutations in *pbo-4* and *pbo-5* specifically eliminate the posterior body contraction step of the defecation cycle motor program.

Cycle timing, other contractions in the motor program, and body-muscle function during locomotion are normal, suggesting that the mutations do not cause general defects in the health of the intestine or muscle but, rather, are specifically involved in signaling between the intestine and the muscle. The simplest model is that protons released by the putative PBO-4 Na^+/H^+ exchanger activate the PBO receptor composed of PBO-5 and PBO-6; activation of this cation channel in turn depolarizes the cell and causes muscle contraction. This model is based on the following observations. First, the putative PBO-4 Na^+/H^+ exchanger is positioned to mediate communication with the muscles. PBO-4 is expressed in the posterior cells of the intestine, which act as the timekeeper for the defecation cycle (Dal Santo et al., 1999; Espelt et al., 2005), and the exchanger is localized to basolateral surface juxtaposed to the overlying body muscles. Second, PBO-4 mediates a transient acidification of the extracellular space preceding the posterior body contraction. Third, uncaging H^+ ions in vivo is sufficient to activate normal posterior body contraction in wild-type or *pbo-4* animals. Fourth, uncaged protons cannot bypass the *pbo-5* defect, demonstrating that PBO-5 is a component of a specific proton receptor on the responding cell.

Protons: A Transmitter in *C. elegans*

In 1958, Paton set out five criteria for admission of a molecule into the pantheon of neurotransmitters (Paton, 1958). Some of these rules have been set aside to accommodate gaseous and peptide transmitters (Baranano et al., 2001; Hyman, 2005); nevertheless, these rules provide a useful framework for considering whether a molecule acts as a neurotransmitter. An updated version (Cowan et al., 2001) of these rules include the following: (1) the chemical must be present in the signaling cell, (2) stimulation of the cell results in the release of the chemical, (3) there will be mechanisms for inactivating the transmitter, (4) the chemical must act on specific receptors on the responding cell, (5) exogenous application of the chemical must mimic the endogenous response, and (6) blocking the receptor blocks the activity of the neurotransmitter. In *C. elegans*, protons possess the attributes of a transmitter for muscle contraction. First, protons are found in all cells. Second, acidification of the extracellular space immediately precedes the posterior contraction. Third, although there is not a specific mechanism for clearing or depleting protons in the coelomic space, diffusion and biological buffers are likely to rapidly neutralize changes in pH. Fourth, protons act on a specific ligand-gated receptor, composed of the PBO-5 and PBO-6 proteins, which are localized to the posterior body muscles. Fifth, application of protons by releasing caged H^+ ions stimulates the posterior body contraction. Sixth, genetic disruption of the receptor blocks the stimulation of muscle contraction by uncaged protons.

Neurotransmitters, of course, are released from neurons, whereas the H^+ ion signal that we describe arises from the intestine. Thus, these experiments demonstrate that H^+ ions are acting as a transmitter rather than a neurotransmitter. However, other Na^+/H^+ ion exchangers (Nehrke and Melvin, 2002) and the acid-sensitive receptor subunit PBO-5 are expressed in neurons. Thus, protons might act as a neurotransmitter at central synapses in *C. elegans*.

Consistent with a broader role for protons as intercellular messengers, a large family of proton-gated channels, termed the acid-sensing ion channels (ASICs), has been identified (Waldmann and Lazdunski, 1998). The ASICs are expressed in both the central and peripheral nervous system. For the most part these receptors are tuned to high-acid environments and are noxious chemical receptors (Waldmann et al., 1997); however, studies indicate that some of these receptors may respond to physiological pH changes and act in intercellular signaling (Wemmie et al., 2002). Specifically, deletion of the mouse ASIC1 gene leads to deficits in learning and memory, suggesting H^+ ion signaling is not confined to sensing noxious environments but is also important in central nervous system function (Wemmie et al., 2002). The source of H^+ ions that activate the ASIC channels in the central nervous system is unknown. While repeated synaptic vesicle exocytosis may provide a limited supply of protons, other sources of “quick protons” such as Na^+/H^+ exchangers are attractive candidates for ASIC channel activation (Kaila and Ransom, 1998; Krishtal, 2003). Further studies may demonstrate that Na^+/H^+ ion exchangers function for the release of H^+ ions acting as a neurotransmitter at central synapses in vertebrates.

EXPERIMENTAL PROCEDURES

Strains and Genetics

Standard methods for maintaining *C. elegans* strains were used (Brenner, 1974). Bristol strain N2 was used as the wild-type, and all animals were grown at room temperature (22.5°C).

Genetic Analysis and Phenotypic Characterization

pbo-4 alleles *n2658* and *sa300* were identified in EMS screens (E.M.J. and H.R. Horvitz, unpublished data; J. Thomas, unpublished data), *ox10* was identified in a diepoxybutane screen, and *ok583* was identified in a UV/TMP screen (Knockout Consortium). Complementation tests confirmed that *n2658*, *ox10*, and *sa300* are alleles of the same gene. *n2658* was mapped to a chromosome using the following mapping strains: EG1000 *dpy-5(e61) I*; *rol-6(e187) II*; *lon-1(e1820) III* and MT464 *unc-5(e53) IV*; *dpy-119(e224) V*; *lon-2(e678) X*. Fine mapping on the X chromosome was performed using the following strains: EG1040 *unc-2(ox2) dpy-6(e14) egl-15(n484)*, MT3001 *dpy-6(e14) egl-15(n484)*, EM327 *unc-115(e2225) vab-3(e648)*, and JT6885 *unc-115(e2225) daf-12(m20) daf-11(m84)*.

pbo-5 alleles (*n2331 dm*, *ox7 dm*, *ox4*, *ox5*, *ox9*, *n2303*, *n2330*, *sa242*, *sa243*, and *sa297*) were identified in EMS (ethyl methanesulfonate) screens for defecation-cycle defective mutants. Additional *pbo-5* alleles (*ox24*, *ox26*, *ox27*, *ox30*, *ox32*, *ox34*, *ox35*, *ox36*, *ox38*, and *ox39*) were identified in an EMS screen for suppressors of the dominant *pbo-5(n2331sd)* posterior body cramp. *pbo-5* alleles were subsequently mapped to a chromosome using the mapping strains: EG1000 *dpy-5(e61) I*; *rol-6(e187) II*; *lon-1(e1820) III* and EG1020 *bli-6(sc16) IV*; *dpy-11(e224) V*; *lon-2(e678) X*. Fine mapping on chromosome V was done with the following strains: MT6931 *egl-8(n2659) dpy-11(e224)*, MT2564 *sqt-3(sc63) him-5(e1467) unc-76(e911)*, MT1505 *dpy-21(e459) unc-51(e369)*, JK1520 *fog-2(q71) pha-4(q496)/stu-3(q265) rol-9(sc148)*, JK1655 *unc-51(e1189) pha-4(q506) rol-9(sc148)/fog-2(q71)*, SM3 *fog-2(q71) rol-9(sc148) pha-4(q500)/stu-3(q265)*, MT6025 *lin-31(n301) III*; *dpy-9(e12) IV*; *unc-51(e369) V*, and MT6185 *dpy-1(e1) III*; *unc-34(e566) V*.

The defecation cycle of day 1 adult animals was scored for 11 cycles from at least 5 individual animals for cycle time and each step of the motor program. Error bars represent SEM.

Transformation Rescue and Cloning

Transgenic strains were generated by standard microinjection techniques (Mello et al., 1991). Rescue of *pbo-4(n2658)* mutants was obtained by

coinjecting the cosmid K09C8 at 20ng/ μ l with 50 ng/ μ l pTG96, a plasmid that contains *sur-5::GFP* as a cotransformation marker. The *pbo-4* genomic subclone (pPD58) was created by ligating an 8.5 kb *AgeI* restriction fragment from cosmid K09C8 into pLitmus 28. pPD58 (20 ng/ μ l) was coinjected with *Pmyo-2::GFP* (2 ng/ μ l) and 1 kb plus DNA Ladder (Invitrogen) (78 ng/ μ l) into *pbo-4(ok583)* animals. Stable lines (*oxEx582*) were obtained, which were completely rescued for posterior body contraction.

Complementary cDNAs of the *pbo-4* transcript were obtained by RT-PCR of wild-type N2 RNA. The 5' *trans*-spliced sequence was obtained by PCR amplification with an SL1 primer and a gene-specific primer. The 3' sequence was obtained by PCR amplification with an oligo-dT primer (GIBCO) and a gene-specific primer. Error-free clones of these PCR products were identified to generate a full-length *pbo-4* cDNA.

To identify the molecular lesions *n2658*, *sa300*, and *ox10*, we sequenced PCR products containing the K09C8.1 predicted open-reading frame from worms of each genotype. The *ok583* allele was isolated by the *C. elegans* Knockout Consortium.

YACs, cosmids, plasmids, and PCR products were prepared and injected into *pbo-5* mutants by standard techniques. YAC deletions were generated by PCR-mediated gene disruption (Brachmann et al., 1998). DNA from mutant strains was prepared and amplified by single-worm PCR to determine the nature of the molecular lesions. Deletion alleles were further characterized by PCR; point mutations were directly sequenced by an automated sequencing machine (Applied Biosystems).

The sequence of the *pbo-5* transcript was determined by reverse transcription of wild-type mRNA followed by PCR amplification (RT-PCR) and direct sequencing. The 5' *trans*-spliced sequence was obtained by PCR amplification using an SL1 primer and a nested, gene-specific primer in the second exon. The 3' sequence was obtained by PCR amplification with nested primers in the third predicted exons and with an oligo-dT primer. PCR products were cloned into the pCR2.1 TA cloning vector (Invitrogen), and a full-length error-free clone pPD68 was generated. For rescue of the *pbo-5* mutant phenotype, a *pbo-5* minigene construct was made containing the Y44A6E.1 cDNA fused to 4.4 kb of sequences upstream of the second exon.

pbo-6 cDNAs were isolated by RT-PCR from polyA⁺ mRNA isolated from wild-type young-adult hermaphrodites. We determined the 5' end of the gene by circular RACE (Maruyama et al., 1995). The 3' end of the gene was based on computer prediction and sequence similarity to *pbo-5*. To isolate full-length cDNAs, oligonucleotide primers were designed to the 5' and 3' untranslated regions of *pbo-6*. PCR products were cloned into pCR2.1, and subsequent products were sequenced to generate a full-length error-free *pbo-6* cDNA.

GFP Expression Constructs

The full-length supercliptic pHluorin-GFP fusion (pAB16) was generated by ligating an 8.5 kb restriction fragment from pPD58 into pCR Blunt (Invitrogen). PCR primers with engineered *Scal* restriction sites were used to PCR amplify the supercliptic GFP coding region from the vector pIA3 (Sankaranarayanan and Ryan, 2000). The 5.8 kb *pbo-4* subclone was linearized with *Scal* and dephosphorylated, using Antarctic phosphatase (NEB). The supercliptic GFP open-reading frame with *Scal* ends was ligated into the linearized plasmid. pAB16 was injected into *pbo-4(ok583)* mutants at 20 ng/ μ l with *Pmyo-2::GFP* at 2 ng/ μ l and 1 kb DNA Ladder (Invitrogen) at 78 ng/ μ l. Stable transgenic lines (EG3325 *pbo-4(ok583)*; *oxEx584* and EG3326 *pbo-4(ok583)*; *oxEx585*) were obtained that exhibited GFP expression on the basolateral surface of the posterior intestine. These animals were also rescued for posterior body contraction. In order to image pHluorin in the *pbo-5* mutant background, a stable transgenic line (EG4178 *pbo-5(ox4)*; *oxEx784*) was generated by injecting pAB16 into *pbo-5(ox4)* mutants at 10 ng/ μ l with *Pmyo-2::GFP* at 1 ng/ μ l and *lin-15(+)* plasmid DNA at 90 ng/ μ l.

The vitellogenin promoter-driven supercliptic GFP fusion (pWD149) was generated by PCR of the pHluorin::GFP fusion from pAB16 using primers that introduce *NcoI* and *SphI* sites flanking the gene. This PCR fragment was cloned into a plasmid pGEM-Pvit-2 (courtesy of Maureen Peters) carrying the promoter for the vitellogenin gene, *vit-2*. pWD149 was injected into *pbo-4(n2658)* mutants at 10 ng/ μ l with *Pmyo-2::GFP* at 1 ng/ μ l and *lin-15(+)* plasmid DNA at 90 ng/ μ l. Stable transgenic lines (EG4077 *pbo-4(n2658)*; *oxEx770*)

were obtained that exhibited dim GFP expression in all intestinal cells of 1-day-old adults and bright expression in older animals. Young adults exhibited rescue; old animals with high PBO-4 expression exhibited defects in the posterior body contraction, perhaps due to desensitization of PBO-5.

To image pHluorin in a *pbo-4* mutant background, a nonrescuing version of pAB16 was generated by deleting the cytoplasmic C terminus of PBO-4 after amino acid 509 (immediately following transmembrane 12). pAB16 was digested with *PmeI* and *BstZ17I* and religated to produce pWD153. A stable transgenic line was created (EG4176 *pbo-4(n2658)*; *oxEx782*) by injecting *pbo-4(n2658)* mutants with pWD153 at 10 ng/ μ l, *Pmyo-2::GFP* at 1 ng/ μ l, and *lin-15(+)* plasmid DNA at 90 ng/ μ l.

The *pbo-5* transcriptional reporter construct contains a 3.8 kb PCR-amplified fragment upstream of the translational start codon fused to the GFP open-reading frame, followed by a stop codon and the polyadenylation site from the *unc-54* gene (pPD54). The *pbo-6* transcriptional reporter construct contains a 4.0 kb PCR-amplified promoter region fused to the GFP open-reading frame followed by a stop codon and the polyadenylation site from the *unc-54* gene (pPD72). These GFP constructs were injected into *lin-15(n765ts)* animals at 10 ng/ μ l along with *lin-15(+)* (pL15EK) as a cotransformation marker at 30 ng/ μ l (Clark et al., 1994) and 1 kb+ DNA ladder at 70 ng/ μ l. Stable transgenic lines were obtained that expressed GFP in the posterior body wall muscles for *pbo-5::gfp* (EG2599 *lin-15(n765ts)*; *oxEx355*) and for *pbo-6::gfp* (EG3322 *lin-15(n765ts)*; *oxEx581*).

pHluorin Imaging

Young-adult animals were immobilized with cyanoacrylate glue on an agarose pad formed on a standard microscope slide. Animals were glued along the length of one side of the body with an effort to leave the very posterior end free to contract. To promote pharyngeal pumping, a necessary activity needed for posterior body contractions, animals were rinsed with 10 mM serotonin (Sigma) and covered with a cover glass, and the edges were sealed with Vaseline. This preparation enabled us to clearly visualize acid transients produced by pHluorin::PBO-4 quenching with a high numerical aperture objective (63 \times , 1.4 N.A. plan apochromat objective [Zeiss]) in wide field on an inverted microscope (iMIC, TILL Photonics). While serotonin increased the likelihood of capturing a pBoc event in rescued animals during the recording period, serotonin is known to produce irregularities in the periodicity of the cycle (E.M.J., unpublished data). This combined with the glued restraint of the animals under a coverslip; we did not expect to see regular periodic cycles. However, we did observe 3 of 18 6 min recordings with astonishing \sim 50 s periodic events. Animals expressing PBO-4::pHluorin were excited with a 488 ± 15 nm light from a monochromator (Polychrome V, TILL Photonics) with a 50 ms exposure time at 10 Hz. Individuals were typically recorded over a period of 6 min. Images were recorded with 4 \times 4 binning on a 14 bit cooled-CCD camera (Andor Technology).

pHluorin Image Analysis

Regions of interest were defined as an area slightly larger than the posterior intestine cells expressing PBO-4::pHluorin in the first frame of the image sequence. Mean pixel intensity of the ROI was computed in each frame of the image sequence using TILLvisiON (TILL Photonics). Over the 6 min acquisition period, an exponential decrement due to photobleaching was observed (\sim 20% of the initial fluorescence was lost at the end of a 6 min session). To measure relative amplitudes of fluorescence changes, the effect of photobleaching was removed by normalizing the baseline to the exponential decline using Igor Pro (Wavemetrics). Corrected traces were further analyzed to measure event amplitude, rise time, and decay using an event detection program (MiniAnalysis, Synaptosoft). Statistical tests were performed using InStat (GraphPad). To identify characteristic posterior body contractions, image sequences were manually inspected. If motion of any kind was observed, the frame in which the motion initiated was noted and compared to the quantitative time course. pHluorin (nonmotion-induced) events were downwardly directed with a fast rise time and slow exponential decay. Spurious motion of the tail could be seen in quantitative time courses, as events that were both positively and negatively directed with irregular kinetics.

Electrophysiology of PBO-5 and PBO-6

To generate plasmid constructs for *Xenopus* oocyte expression, we subcloned full-length error-free cDNAs into the pSGEM expression vector (Villmann et al., 1997). The *pbo-5* expression vector was constructed by cutting the pPD70 plasmid with restriction enzymes SacII and EagI, then using T4 DNA polymerase to blunt the ends. Cut products were gel purified (QIAGEN) and religated using T4 DNA ligase (Promega) to create the plasmid pAB20. The PBO-6 expression construct was generated from a previously sequenced error-free cDNA (M. Peter, unpublished data). A blunt-end cDNA fragment was cloned into the HincII site of the pSGEM expression vector to produce pAB21.

Capped RNA was prepared using the T7 mMessage mMachine kit (Ambion). *Xenopus* oocytes were collected and injected with 25 ng each of PBO-5 and/or PBO-6 cRNA and two-electrode voltage clamp recordings were performed 3–5 days postinjection. For most experiments, the standard bath solution for dose-response and control I-V experiments was Ringer's (in mM): 115 NaCl, 1.8 BaCl₂, 10 Bis-Tris Propane (pH 7.4 acetic acid). For dose-response experiments, each oocyte was subjected to a 5 s application of test pH (7.0–5.0) with 2 min of pH 7.4 wash between test applications. Buffers used were either Bis-Tris Propane (1,3-Bis[tris(hydroxymethyl)methylamino]propane), MES (2-(N-Morpholino)ethanesulfonic acid) or HEPES (N-2-Hydroxyethylpiperazine-N'-2-ethanesulfonic acid). Before each experiment, at least two control oocytes were voltage clamped at –60 mV and maximal pH 6.0 test pulses were applied to ensure that individual batches of oocytes did not express endogenous proton-activated channels that could obscure analysis.

Data Analysis

Data acquisition and analysis were performed using Axograph (Axon Instruments) software, and curve fitting and statistical analysis were performed with Prism (Graphpad). Dose-response curves from individual oocytes were normalized to the maximum and minimum values and averaged for at least 11 oocytes. Normalized data were fit to the four-parameter equation derived from the Hill equation: $Y = \text{Min} + (\text{Max} - \text{Min}) / (1 + 10^{-(\text{LogEC}_{50} - X)/n_H})$, where *Max* is the maximal response, *Min* is the response at the lowest drug concentration, *X* is the logarithm of agonist concentration, EC₅₀ is the half-maximal response, and *n_H* is the Hill coefficient. Error bars represent the standard error of the mean.

Flash Photolysis of Caged H⁺

Adult animals were injected with 0.1 mg/ml NPE-caged proton (2-hydroxyphenyl-1-(2-nitrophenyl)ethyl phosphate, sodium salt, and 0.1 mg/ml FITC-dextran (fluorescein-dextran, sodium salt, 10,000 MW) as a coinjection marker. The caged-H⁺ ion and FITC-dextran were dissolved in 5 mM Na⁺ phosphate (pH 7.0). Animals were mounted on an agarose pad and injected in the coelomic space. Injections were done adjacent to the vulva to avoid damaging the posterior body muscles with the needle. Successful injections were determined by scoring for the coinjection marker FITC-dextran; these animals were allowed to recover for 25–30 min in the dark on nematode growth plates. Animals were observed for one to two defecation cycles to determine if the animal was behaving normally. Next, we either mounted the animal on a cooled 2% agarose pad covered with bacteria or kept the animals on agarose plates with bacteria. A modified DAPI filter set that allowed <360 nm and a manual shutter were used to apply UV light to the injected animal for 1–3 s. Digital video recordings were acquired directly to a computer through a cooled CCD camera.

Quantification was performed offline by reviewing recorded video using iMovie (Apple). Movies were played in slow motion, and still frames were saved for individual animals immediately preceding the flash, immediately after the flash, and after recovery. To quantify the mean contractile distance, we measured from the vulva to the posterior tip of the tail for each saved frame. We used the vulva as a landmark that would be consistent from animal to animal. Distances were measured using ImageJ (NIH). At least five animals were quantified for each genotype.

Supplemental Data

Supplemental Data include six figures, two tables, Supplemental Experimental Procedures, and two movies and can be found with this article online at <http://www.cell.com/cgi/content/full/132/1/149/DC1/>.

ACKNOWLEDGMENTS

We thank the members of the Jorgensen lab, Drs. Doju Yoshikami, Mike Sanguinetti, and David Piper for technical advice and critical readings of this manuscript. Shigeki Watanabe provided the electron micrograph of the intestinal-muscular junction. We'd like to thank Maureen Peters for mapping and sequencing the *ox10* allele and the pGEM-pvit-2 plasmid. Jim Thomas provided the *sa300* allele, and the *Caenorhabditis* Genetics Center supplied *ok583*. Keith Nehrke generously provided the PIA3 plasmid. The *Caenorhabditis* Genetics Center provided some strains and the *C. elegans* genome sequencing consortium for cosmid DNA. Dr. Michael Hollmann generously provided the pSGEM oocyte expression vector. We thank Dr. Andrew Fire for GFP plasmids.

Received: November 21, 2005

Revised: July 7, 2007

Accepted: October 25, 2007

Published: January 10, 2008

REFERENCES

- Aharonovitz, O., Zaun, H.C., Balla, T., York, J.D., Orlowski, J., and Grinstein, S. (2000). Intracellular pH regulation by Na⁺/H⁺ exchange requires phosphatidylinositol 4,5-bisphosphate. *J. Cell Biol.* 150, 213–224.
- Baranano, D.E., Ferris, C.D., and Snyder, S.H. (2001). Atypical neural messengers. *Trends Neurosci.* 24, 99–106.
- Bell, S.M., Schreiner, C.M., Schulteis, P.J., Miller, M.L., Evans, R.L., Vorhees, C.V., Shull, G.E., and Scott, W.J. (1999). Targeted disruption of the murine *Nhe1* locus induces ataxia, growth retardation, and seizures. *Am. J. Physiol.* 276, C788–C795.
- Betz, H. (1990). Ligand-gated ion channels in the brain: the amino acid receptor superfamily. *Neuron* 5, 383–392.
- Bocquet, N., Prado de Carvalho, L., Cartaud, J., Neyton, J., Le Poupon, C., Taly, A., Grutter, T., Changeux, J.P., and Corringer, P.J. (2007). A prokaryotic proton-gated ion channel from the nicotinic acetylcholine receptor family. *Nature* 445, 116–119.
- Brachmann, C.B., Davies, A., Cost, G.J., Caputo, E., Li, J., Hieter, P., and Boeke, J.D. (1998). Designer deletion strains derived from *Saccharomyces cerevisiae* S288C: a useful set of strains and plasmids for PCR-mediated gene disruption and other applications. *Yeast* 14, 115–132.
- Brejci, K., van Dijk, W.J., Klaassen, R.V., Schuurmans, M., van Der Oost, J., Smit, A.B., and Sixma, T.K. (2001). Crystal structure of an ACh-binding protein reveals the ligand-binding domain of nicotinic receptors. *Nature* 411, 269–276.
- Brenner, S. (1974). The genetics of *Caenorhabditis elegans*. *Genetics* 77, 71–94.
- Clark, S.G., Lu, X., and Horvitz, H.R. (1994). The *Caenorhabditis elegans* locus *lin-15*, a negative regulator of a tyrosine kinase signaling pathway, encodes two different proteins. *Genetics* 137, 987–997.
- Counillon, L., and Pouyssegur, J. (2000). The expanding family of eucaryotic Na⁺/H⁺ exchangers. *J. Biol. Chem.* 275, 1–4.
- Cowan, W.M., Sèudhof, T.C., Stevens, C.F., and Howard Hughes Medical Institute. (2001). *Synapses* (Baltimore: Johns Hopkins University Press).
- Croll, N.A. (1975). Behavioural analysis of nematode movement. *Adv. Parasitol.* 13, 71–122.
- Dal Santo, P., Logan, M.A., Chisholm, A.D., and Jorgensen, E.M. (1999). The inositol trisphosphate receptor regulates a 50-second behavioral rhythm in *C. elegans*. *Cell* 98, 757–767.
- Del Castillo, J., Nelson, T.E., Jr., and Sanchez, V. (1962). Mechanism of the increased acetylcholine sensitivity of skeletal muscle in low pH solutions. *J. Cell. Comp. Physiol.* 59, 35–44.
- Denker, S.P., Huang, D.C., Orlowski, J., Furthmayr, H., and Barber, D.L. (2000). Direct binding of the Na⁺-H exchanger NHE1 to ERM proteins regulates the cortical cytoskeleton and cell shape independently of H⁺ translocation. *Mol. Cell* 6, 1425–1436.

- Espelt, M.V., Estevez, A.Y., Yin, X., and Strange, K. (2005). Oscillatory Ca²⁺ Signaling in the Isolated *Caenorhabditis elegans* Intestine: Role of the Inositol-1,4,5-trisphosphate Receptor and Phospholipases C beta and gamma. *J. Gen. Physiol.* *126*, 379–392.
- Giffard, R.G., Monyer, H., Christine, C.W., and Choi, D.W. (1990). Acidosis reduces NMDA receptor activation, glutamate neurotoxicity, and oxygen-glucose deprivation neuronal injury in cortical cultures. *Brain Res.* *506*, 339–342.
- Hyman, S.E. (2005). Neurotransmitters. *Curr. Biol.* *15*, R154–R158.
- Kaila, K. (1994). Ionic basis of GABAA receptor channel function in the nervous system. *Prog. Neurobiol.* *42*, 489–537.
- Kaila, K., and Ransom, B.R. (1998). pH and brain function (New York: Wiley-Liss).
- Karlin, A., and Akabas, M.H. (1995). Toward a structural basis for the function of nicotinic acetylcholine receptors and their cousins. *Neuron* *15*, 1231–1244.
- Krishtal, O. (2003). The ASICs: signaling molecules? Modulators? *Trends Neurosci.* *26*, 477–483.
- Lin, X., and Barber, D.L. (1996). A calcineurin homologous protein inhibits GTPase-stimulated Na-H exchange. *Proc. Natl. Acad. Sci. USA* *93*, 12631–12636.
- Maruyama, I.N., Rakow, T.L., and Maruyama, H.I. (1995). cRACE: a simple method for identification of the 5' end of mRNAs. *Nucleic Acids Res.* *23*, 3796–3797.
- Mello, C.C., Kramer, J.M., Stinchcomb, D., and Ambros, V. (1991). Efficient gene transfer in *C.elegans*: extrachromosomal maintenance and integration of transforming sequences. *EMBO J.* *10*, 3959–3970.
- Miesenböck, G., De Angelis, D.A., and Rothman, J.E. (1998). Visualizing secretion and synaptic transmission with pH-sensitive green fluorescent proteins. *Nature* *394*, 192–195.
- Nehrke, K., and Melvin, J.E. (2002). The NHX family of Na⁺-H⁺ exchangers in *Caenorhabditis elegans*. *J. Biol. Chem.* *277*, 29036–29044.
- Norman, K.R., Fazio, R.T., Mellem, J.E., Espelt, M.V., Strange, K., Beckerle, M.C., and Maricq, A.V. (2005). The Rho/Rac-family guanine nucleotide exchange factor VAV-1 regulates rhythmic behaviors in *C. elegans*. *Cell* *123*, 119–132.
- Orlowski, J. (1993). Heterologous expression and functional properties of amiloride high affinity (NHE-1) and low affinity (NHE-3) isoforms of the rat Na/H exchanger. *J. Biol. Chem.* *268*, 16369–16377.
- Orlowski, J., and Grinstein, S. (2004). Diversity of the mammalian sodium/proton exchanger SLC9 gene family. *Pflugers Arch.* *447*, 549–565.
- Ortells, M.O., and Lunt, G.G. (1995). Evolutionary history of the ligand-gated ion-channel superfamily of receptors. *Trends Neurosci.* *18*, 121–127.
- Palma, A., Li, L., Chen, X.J., Pappone, P., and McNamee, M. (1991). Effects of pH on acetylcholine receptor function. *J. Membr. Biol.* *120*, 67–73.
- Pang, T., Su, X., Wakabayashi, S., and Shigekawa, M. (2001). Calcineurin homologous protein as an essential cofactor for Na⁺/H⁺ exchangers. *J. Biol. Chem.* *276*, 17367–17372.
- Paton, W.D. (1958). Central and synaptic transmission in the nervous system; pharmacological aspects. *Annu. Rev. Physiol.* *20*, 431–470.
- Peters, M.A., Teramoto, T., White, J.Q., Iwasaki, K., and Jorgensen, E.M. (2007). A Calcium Wave Mediated by Gap Junctions Coordinates a Rhythmic Behavior in *C. elegans*. *Curr. Biol.* *17*, 1601–1608.
- Sankaranarayanan, S., and Ryan, T.A. (2000). Real-time measurements of vesicle-SNARE recycling in synapses of the central nervous system. *Nat. Cell Biol.* *2*, 197–204.
- Smart, T.G., and Constanti, A. (1982). A novel effect of zinc on the lobster muscle GABA receptor. *Proc. R. Soc. Lond. B. Biol. Sci.* *215*, 327–341.
- Takeuchi, A., and Takeuchi, N. (1967). Anion permeability of the inhibitory post-synaptic membrane of the crayfish neuromuscular junction. *J. Physiol.* *191*, 575–590.
- Thomas, J.H. (1990). Genetic analysis of defecation in *Caenorhabditis elegans*. *Genetics* *124*, 855–872.
- Traynelis, S.F., and Cull-Candy, S.G. (1990). Proton inhibition of N-methyl-D-aspartate receptors in cerebellar neurons. *Nature* *345*, 347–350.
- Unwin, N. (1993). Nicotinic acetylcholine receptor at 9 Å resolution. *J. Mol. Biol.* *229*, 1101–1124.
- Villmann, C., Bull, L., and Hollmann, M. (1997). Kainate binding proteins possess functional ion channel domains. *J. Neurosci.* *17*, 7634–7643.
- Wakabayashi, S., Bertrand, B., Ikeda, T., Pouyssegur, J., and Shigekawa, M. (1994). Mutation of calmodulin-binding site renders the Na⁺/H⁺ exchanger (NHE1) highly H⁺-sensitive and Ca²⁺ regulation-defective. *J. Biol. Chem.* *269*, 13710–13715.
- Wakabayashi, S., Ikeda, T., Iwamoto, T., Pouyssegur, J., and Shigekawa, M. (1997). Calmodulin-binding autoinhibitory domain controls “pH-sensing” in the Na⁺/H⁺ exchanger NHE1 through sequence-specific interaction. *Biochemistry* *36*, 12854–12861.
- Wakabayashi, S., Pang, T., Su, X., and Shigekawa, M. (2000). A novel topology model of the human Na⁽⁺⁾/H⁽⁺⁾ exchanger isoform 1. *J. Biol. Chem.* *275*, 7942–7949.
- Waldmann, R., and Lazdunski, M. (1998). H⁽⁺⁾-gated cation channels: neuronal acid sensors in the NaC/DEG family of ion channels. *Curr. Opin. Neurobiol.* *8*, 418–424.
- Waldmann, R., Champigny, G., Bassilana, F., Heurteaux, C., and Lazdunski, M. (1997). A proton-gated cation channel involved in acid-sensing. *Nature* *386*, 173–177.
- Wemmie, J.A., Chen, J., Askwith, C.C., Hruska-Hageman, A.M., Price, M.P., Nolan, B.C., Yoder, P.G., Lamani, E., Hoshi, T., Freeman, J.H., Jr., et al. (2002). The acid-activated ion channel ASIC contributes to synaptic plasticity, learning, and memory. *Neuron* *34*, 463–477.
- Zha, X.M., Wemmie, J.A., Green, S.H., and Welsh, M.J. (2006). Acid-sensing ion channel 1a is a postsynaptic proton receptor that affects the density of dendritic spines. *Proc. Natl. Acad. Sci. USA* *103*, 16556–16561.

Supplemental Data

Protons Act as a Transmitter for Muscle Contraction in *C. elegans*

Asim A. Beg, Glen G. Ernstrom, Paola Nix, M. Wayne Davis, and Erik M. Jorgensen

Supplemental Movie Legends

Movie S1. Wild-type GFP_{pH}::PBO-4 Response

Real-time movie of the tail (anterior left, posterior right) of a transgenic animal expressing GFP_{pH}::PBO-4 in the posterior intestine during a fluorescence transient followed by a posterior body contraction (fluorescence is quantitated in Figure 4). Notice the fluorescence intensity decrease (decrease in red) prior to anterior directed contraction characteristic of a posterior body contraction.

Movie S2. GFP_{pH}::PBO-4 response in *pbo-5* mutant

Real-time movie of the tail of a transgenic animal expressing GFP_{pH}::PBO-4 in the posterior intestine in the *pbo-5(ox4)* mutant background. *pbo-5(ox4)* mutants fail to execute posterior body contractions. In this movie, fluorescence decreases with a similar time course as the wild-type response but no posterior body contraction follows.

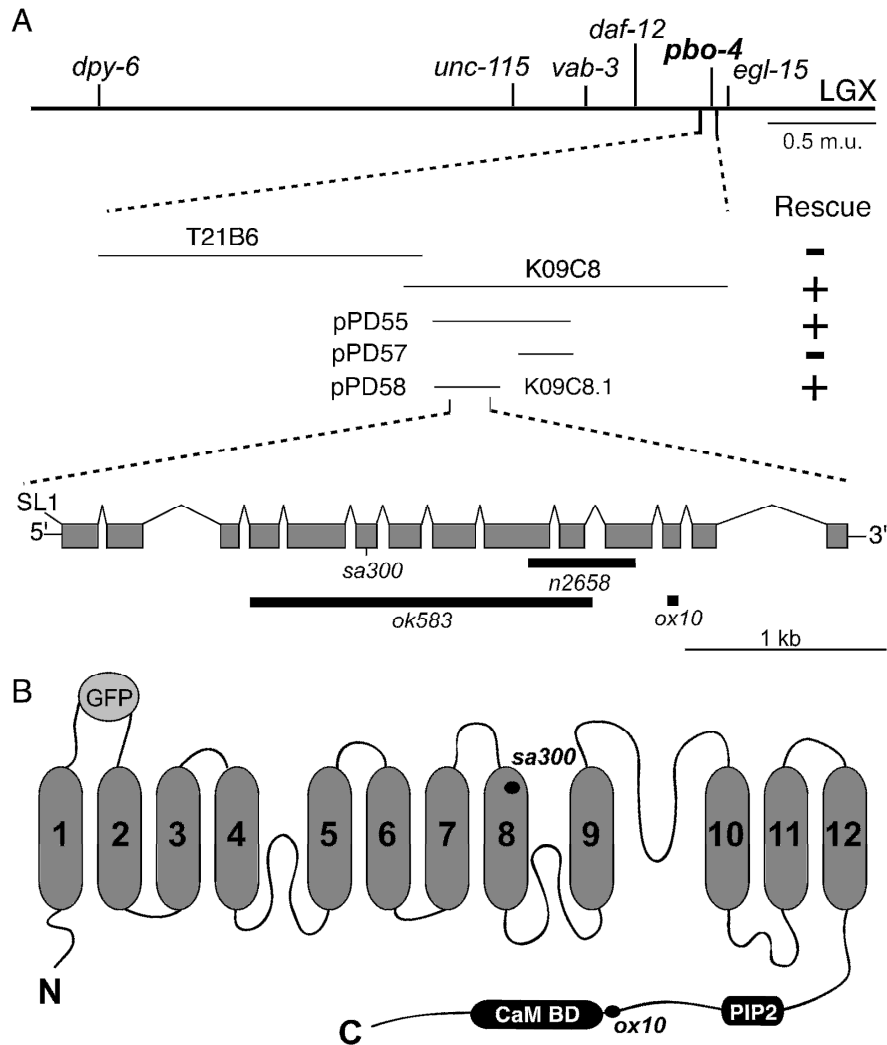


Figure S1. Genetic Mapping and Molecular Cloning of *pbo-4*

(A) Above, the *pbo-4* locus maps between *daf-12* and *egl-15* on the X chromosome, including the cosmids T21B6 and K09C8. Rescue (+) of the posterior body contraction defect by cosmid or subclone is indicated. Below, the exon-intron structure of *pbo-4*. Black bars denote the extent of deletion alleles within the locus.

(B) Predicted PBO-4 protein domains. The predicted protein consists of 12 transmembrane domains, a re-entrant loop between transmembrane domains 9 and 10 and an intracellular carboxy-terminal tail that contains a predicted PIP₂ binding domain, a calmodulin binding domain, and several phosphorylation sites. The insertion of GFP after transmembrane domain 1 in the tagged rescuing construct *oxEx584* is shown.

Figure S2, Beg et al

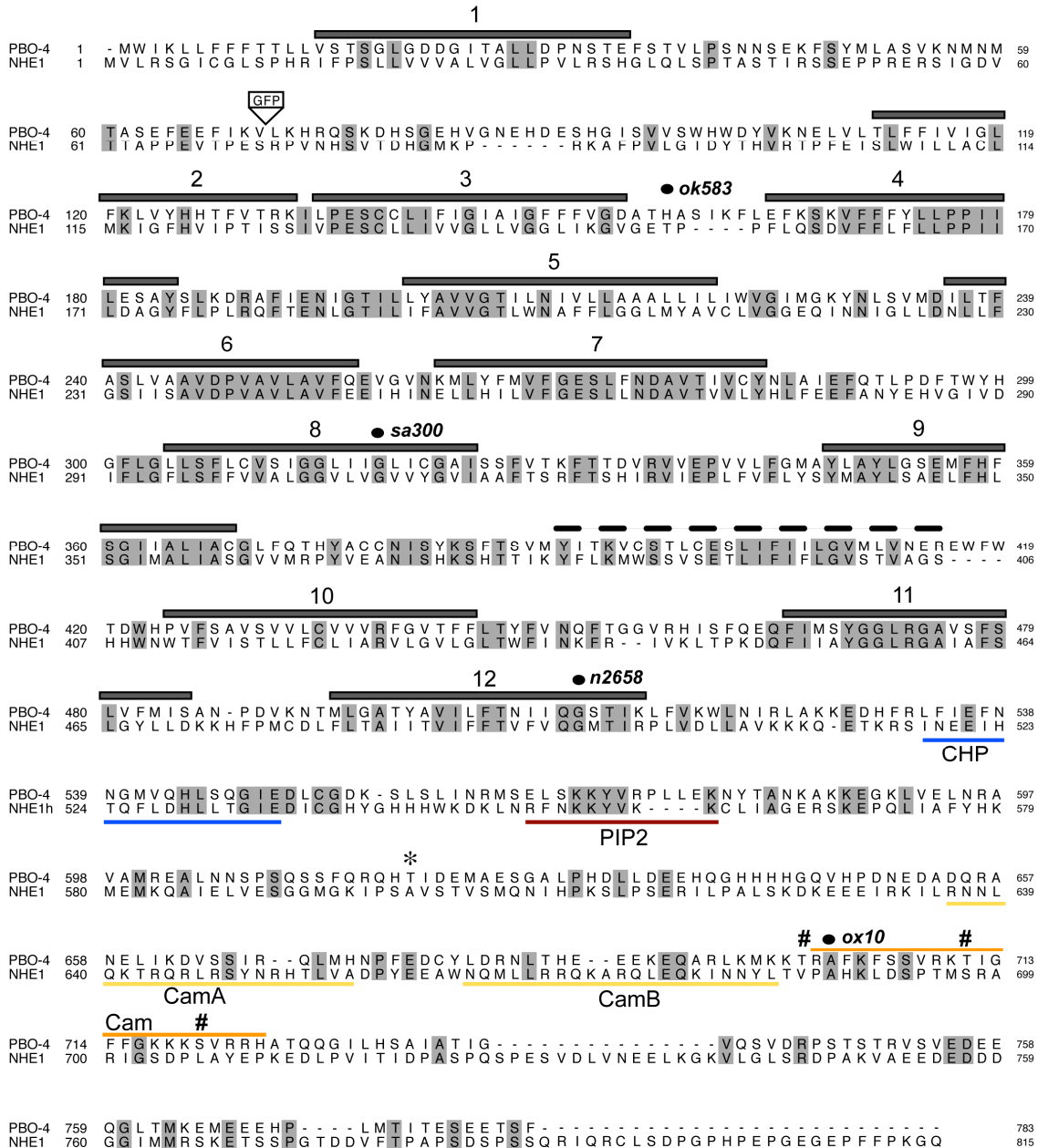


Figure S2. Sequence Alignment of PBO-4 to a Human Na⁺/H⁺ Exchanger
 Deduced polypeptide sequence of PBO-4 aligned with human NHE1 (P19634). Sequences were aligned with ClustalX. Identities are shaded. *pbo-4* mutations are denoted by black circles, for deletion alleles the first affected amino acid is indicated. The black bars indicate predicted transmembrane domains, and the dotted line denotes the re-entrant loop as determined for NHE1 (Wakabayashi et al., 2000). The colored lines demarcate the regulatory elements within the carboxy terminus of PBO-4 and NHE1 (CHP = calcineurin homologous protein binding domain; Cam = calmodulin binding domain; PIP2 = PIP₂ binding domain). ‘Cam’ denotes the putative PBO-4 calmodulin binding domain (orange line) and CamA and CamB are the NHE1 calmodulin binding domains (yellow lines). The position of the GFP insertion is indicated. * marks a predicted CamKII phosphorylation site and # marks predicted PKC phosphorylation sites.

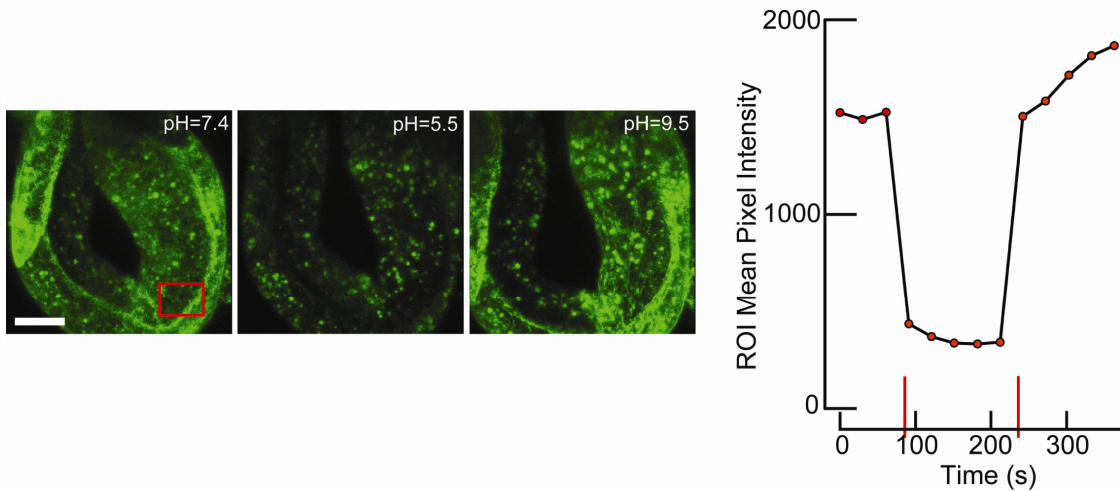


Figure S3. Basolateral Intestine pHluorin is Sensitive to External pH.

Left, confocal images of an intact posterior intestine expressing pHluorin:PBO-4 (EG3325 *pbo-4(ok583); oxEx584[pHluorin::PBO-4; Pmyo-2::GFP]*) exposed to external media superfused at the pH indicated above. Consistent with pHluorin quenching at low pH, intestinal fluorescence is greatly reduced at pH5.5 and increased at pH9.5. Scale bar, 20 μ m. The red box in the first image indicates the region-of-interest where mean pixel intensity was measured. Right, quantitative fluorescence from intestine at left. The first red dash in the graph indicates the time at which saline superfusion was switched from pH7.4 to pH5.5 and the second when switched from pH5.5 to pH9.5.

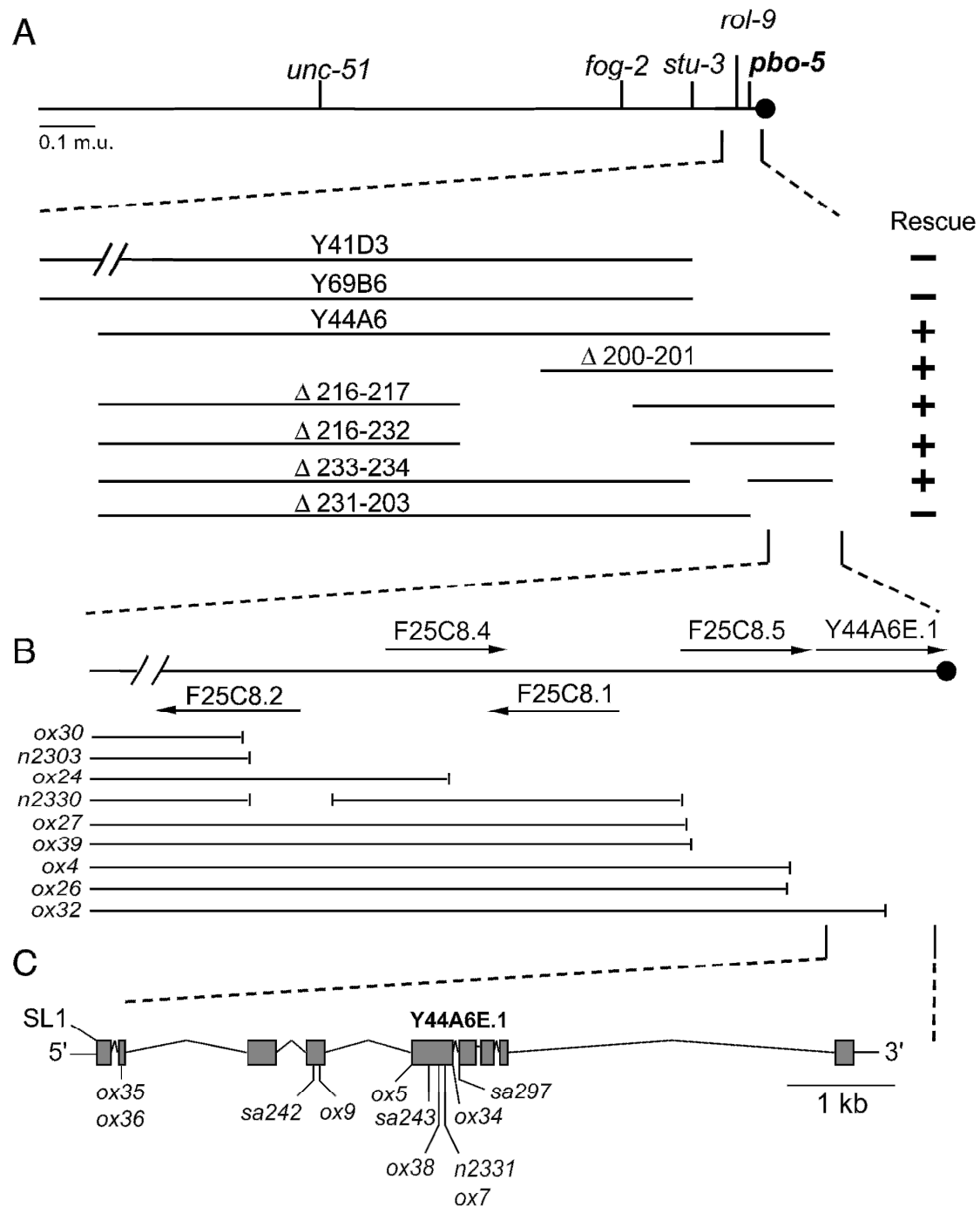


Figure S4. Behavioral Phenotype and Cloning of *pbo-5*

(A) The genomic location of *pbo-5* on chromosome V. The *pbo-5* gene is the last predicted gene on chromosome V, approximately 1.2 kb from the telomere (black circle). Rescue of the posterior body contraction defect by YAC or subclone is indicated (+/-).

(B) Relative position of open reading frames in the *pbo-5* vicinity with approximate end-points of *pbo-5* deletion alleles indicated. A blank represents deleted sequence with respect to the normal end of the chromosome.

(C) Exon-intron structure of the *pbo-5* gene. Positions of mutations in *pbo-5* alleles are shown.

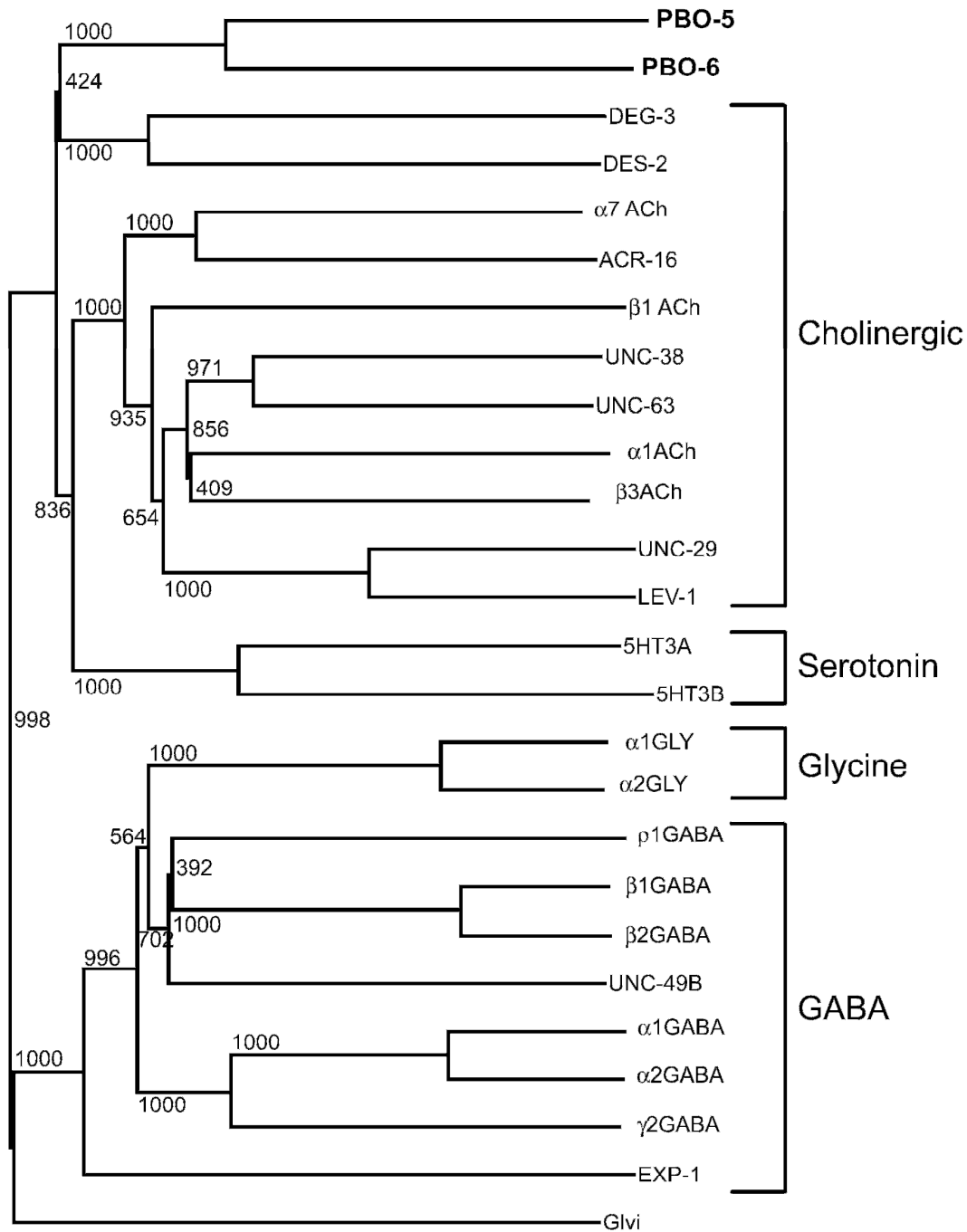


Figure S6. PBO-5 and PBO-6 Phylogenetic Tree

PBO-5 and PBO-6 represent novel ligand-gated ion channel subunits. The PBO-5 and PBO-6 subunits cannot be categorized into one of the four ligand-gated ion channel families based on sequence analysis. Alignments were performed using ClustalX and the bootstrap method and ‘neighbor-joining’ search was used to create the tree. Bootstrap values of 1,000 replicates are indicated on the tree.

Supplemental Experimental Procedures

Evidence that GFP_{pH}::PBO-4 is sensitive to extracellular pH changes: The DNA sequence encoding superecliptic pHluorin (Sankaranarayanan et al., 2000) was inserted into the *pbo-4* gene between predicted membrane domains one and two. Sequence analysis of the PBO-4 peptide predicted that the inserted pHluorin would be exposed to the extracellular side (see Figure 2B in the main text). To test this topological prediction, posterior intestines expressing GFP_{pH}::PBO-4 were imaged when exposed to different extracellular salines buffered to pH=7.4, pH=5.5, and pH=9.5. To prepare animals for imaging, the posterior intestines were exposed to medium (pH 7.4) in a petri dish by puncturing the tails of adult animals with a 28-gauge needle. The hydrostatic pressure of the *C. elegans* body cavity forced a portion of intact, posterior intestine out of the body into the medium. These posterior-punctured animals were transferred to a recording chamber with a cover glass bottom coated with an adhesive substance, Cell-Tak (BD Biosciences) (see Norman et al., 2005). Fluorescence was imaged on an upright LSM 5 PASCAL confocal microscope equipped with a 100x, 1.0 N.A. achroplan water immersion objective. A series of images was acquired every 25.5 seconds as salines at pH=7.4, pH=5.5, and pH=9.5 were sequentially superfused over the exposed posterior intestine. **Figure S3** shows significant fluorescence quenching upon switching to the acidic saline. Consistent with the pH-sensitivity of superecliptic pHluorin, fluorescence intensity recovered to higher levels when the preparation was superfused with alkaline medium (pH=9.5). The fluorescence changes from intact GFP_{pH}::PBO-4 expressing intestine associated with changes in medium pH indicate the pHluorin sensor is sensitive to extracellular pH changes when inserted into PBO-4. Similar responses were seen in two other preparations.

Frequency of observing pBocs associated with a pHluorin event: As described in the Methods, 1-day-old adult animals were prepared for imaging by applying cyanoacrylate glue (NEXABAND, World Precision Instruments, Inc.) along one side of an animal mounted on an agarose pad (see Goodman et al., 1998). To attempt to visualize a posterior body contraction, effort was made to apply glue along the length of the animal except for a small portion of the posterior end. In the strain with the rescuing GFP_{pH}::PBO-4 transgene, 6/15 preparations were glued in such a manner that the tail was mobile just enough to make a posterior body contraction (pBoc) (see **Movie S1** and **Figure S4**). In these preparations where a posterior body contraction could be seen, the posterior body contraction always followed pHluorin quenching with a latency of 2.41 ± 0.44 s, n=6. The start of the characteristic accordion-like posterior body contraction was noted by manually replaying the image sequence where one could advance the video frame-by-frame if needed. There was also sufficient background fluorescence to discern the outline of the tail. Although every posterior body contraction was associated with a pHluorin event, not every pHluorin event recorded was associated with a posterior body contraction: $36 \pm 10\%$, (n=6) of all pHluorin events were associated with a posterior body contraction.

Table S1. Summary of *pbo-4* mutations

Allele	Nucleotide change	Protein change
<i>sa300</i>	GGA → AGA	G 318 R
<i>n2658</i>	ggtattaa (Δ547bp)GACAC	Δ510-639 frameshift 26 a.a...stop
<i>ok583</i>	GCGACTCA(Δ1702bp)aattttt	Δ157-601 frameshift 8 a.a...stop
<i>ox10</i>	GCA → GΔA	A 717 D frameshift 5 a.a...stop

Table S1. Summary of *pbo-4* mutations. The nucleotide and protein change of each *pbo-4* allele.

Table S2. Summary of *pbo-5* mutations

Allele	Mutation	Protein	Exon/Domain
<i>ox35</i>	nonsense	Q 59 stop	2
<i>ox36</i>	nonsense	Q 59 stop	2
<i>sa243</i>	nonsense	W 235 stop	5
<i>n2331dm</i>	missense	L 316 F	5 (M2)
<i>ox7dm</i>	missense	L 316 F	5 (M2)
<i>ox38</i>	missense	T 304 I	5 (M2)
<i>ox34</i>	missense	P 325 L	5 (M2-M3 loop)
<i>sa297</i>	missense	M 342 T	6 (M3)
<i>ox9</i>	missense	H 184 Q	4 (LBD)
<i>sa242</i>	missense	P 181 L	4 (LBD)
<i>ox5</i>	splice		intron 4
<i>n2330, ox4, ox24, ox26, ox27, ox30, ox32, ox39</i>	deletion		

Table S2. Summary of *pbo-5* mutations. The mutation type, resultant protein change and genomic location of each *pbo-5* allele.